

# ***Interactive comments on “Regional-scale Simulations of Fungal Spore Aerosols Using an Emission Parameterization Adapted to Local Measurements of Fluorescent Biological Aerosol Particles” by M. Hummel et al.***

**M. Hummel et al.**

matthias.hummel@kit.edu

## **Anonymous Referee #1**

We thank the reviewer for his/her comments which have improved our manuscript. The comments are listed below in italics.

*In general, the FBAP measurements measure all particles in the range of 2-4µm, however, it the authors assume these are fungal spores. Bacterial agglomerate, as well as giant bacteria and agglomerates of free proteins and amino acids could contribute to this fraction. In this case, the simulations, referring only to fungal spores would not represent this data well. This point should be further addressed and quantified, as the introduction generalizes this issue to the entire PBAP population.*

It is not entirely clear what kind of biological particles dominate FBAP number concentrations. Several field and lab studies show that fungal spores and bacteria cells or bacteria agglomerates can contribute to FBAP concentrations in a size range of 2-4 µm (Pöhlker et al., 2012; Healy et al., 2014; Huffman et al., 2010; Gabey et al., 2013; Robinson et al., 2013). Taking previous studies into account, we conclude that FBAP concentrations shown in this study are dominated by fungal spores, but might also include to some extent contributions of other PBAP. A summary of recent WIBS and UV-APS measurements focusing on this issue is already included in section 2.4.

*For readers not familiar with the measurement techniques, online measurements alone weaken the robustness of the study. If there are previously published works that validate this measurement with more traditional ways such as filters and genomics, please add them to show that this technique is robust and validated. If not – such validation is needed.*

Additional references to previous studies that validate FBAP measurements with traditional techniques are included in section 2.4.

Text added: “At the costal site of Killarney, results of fluorescence and optical microscopy of impacted biological particles reveal that some PBAP, e.g. Spores of *Cladosporium spp.*, which have been frequently observed in many environments, were not correlated to the FBAP concentration (Healy et al., 2014). However, particle size modes of WIBS channel FL2\_280 correlate with the concentration of airborne fungal spores commonly observed at the sampling site (Healy et al., 2014).”

*In general, the authors should expend the experimental section for instrumentation and validations. For instance, what is the sensitivity of the instruments? This could lead to underestimation of biological particle detection.*

Most FBAP measurement data is also shown elsewhere (Schumacher et al., 2013; Toprak and Schnaiter, 2013; Gabey et al., 2011) and some include information about the sensitivity of the instruments. This manuscript is already rather long and its focus is on the comparison of FBAP data to model results. Additional information about the experimental part is contained in other studies (Gabey et al., 2010; Huffman et al., 2010; Pöhlker et al., 2012; Robinson et al., 2013).

*P. 10, line 8: this sentence is inaccurate, as not all proteins will contain fluorophore-containing amino acids.*

This issue is now taken into account and the sentence has been corrected as follows: “The region of excitation near 270 nm includes certain amino acids (e.g. tryptophan) contained in most proteins.”

*The Authors assume that there is no contribution from dust in this size range. Could the authors supply evidence (using back trajectory analysis for example) support this assumption?*

Mineral dust also shows slight fluorescence signals which can result in a detected fluorescence fraction in WIBS instruments between <1% and 5.8% (Gallagher, 2014; Toprak and Schnaiter, 2013). It may therefore interfere with the FBAP signal (Pöhlker et al., 2012; Gabey et al., 2011). Contribution of mineral dust to FBAP concentration can only occur during dust events. For the investigated locations and time periods however, no contribution of desert dust is confirmed by using back trajectories (Figure 1 to Figure 3) by using HYSPLIT (Draxler and Rolph, 2013). All locations mostly show local contributions for the selected test cases. Contribution of soil dust may be part of particles from local sources. Soil dust can be internally mixed with fungal spores or other organic components.

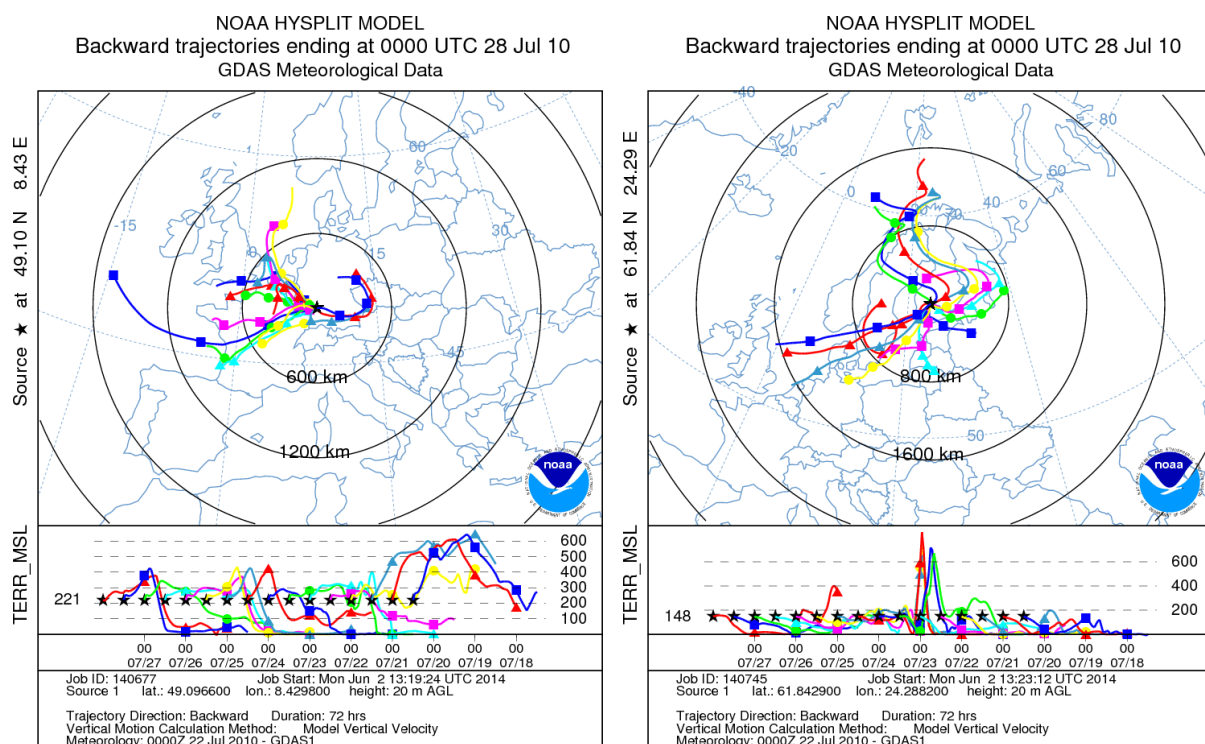


**Figure 1. Back trajectories for the locations Karlsruhe and Hyttiälä at the simulation case during July 2010**

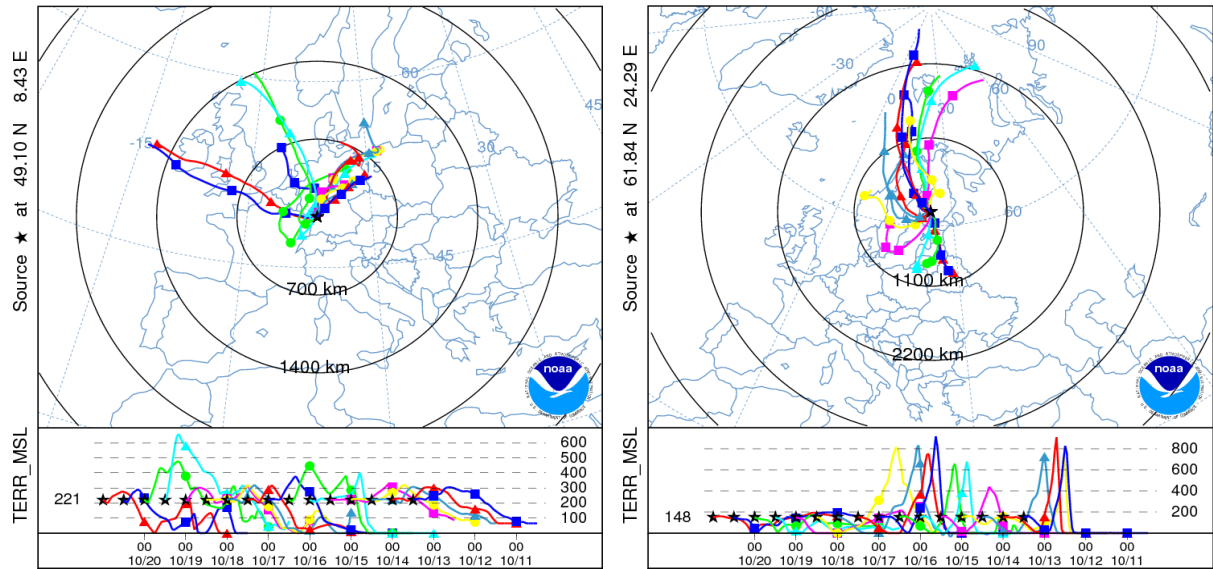


Figure 2. Back trajectories for the locations Karlsruhe and Hyttiälä at the simulation case during October 2010

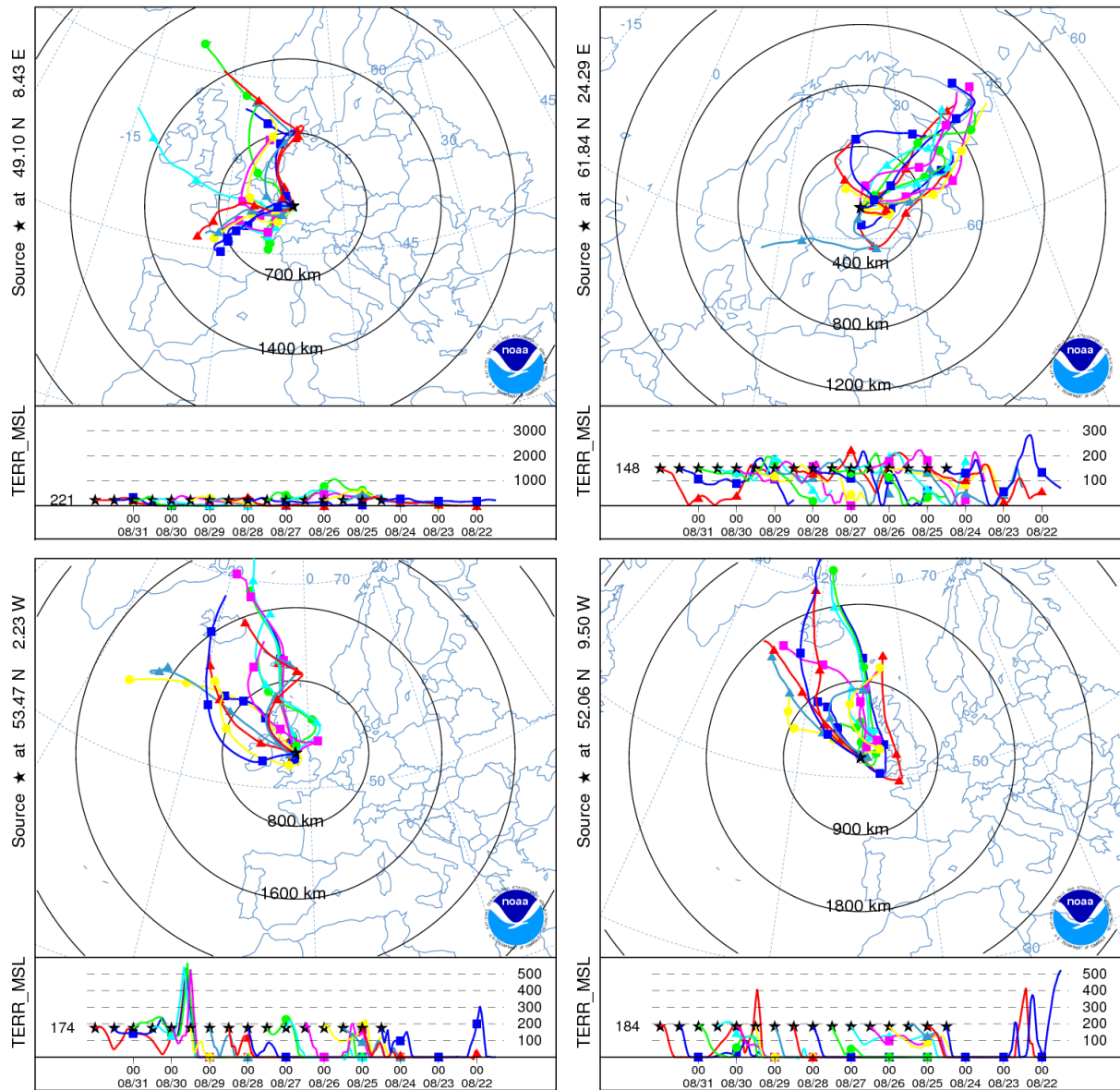


Figure 3. Back trajectories for the locations Karlsruhe, Hyttiälä, Manchester, and Killarney at the simulation case during August 2010

*The two previously published models are based on manitol concentration, which can also indicate on other types of particles, such as vegetation in addition to fungal spores. This may lead to overestimation of bio aerosol loads. This should be mentioned and discussed as one of the factors influencing the difference between models and measurements.*

Heald and Spracklen (2009) use mannitol concentrations that are compiled in Elbert et al. (2007) in order to estimate fungal spore emissions which best represent mean observed concentrations. Additional information about PBAP which are also containing mannitol (i.e. bacteria, algae, lichens, and plant fragments) is now added to the manuscript.

*The authors correct the spores suspension time in the atmosphere to be 4 ¼ [hours]. This significant claim needs to be validated before stated.*

In the updated manuscript version, this statement has been clarified. In order to calculate eq. 7, we need to assume a constant boundary layer residence time, previously called atmospheric lifetime. For a first shot, we used an approximation for atmospheric lifetime found in literature. A first model run with the new emission parameterization (calculated by using  $\tau = 1$  day) revealed that the simulated fungal spore concentrations still underestimates the measured FBAP concentrations, although they are adapted to the measurements. We now calculated a corrected boundary layer residence time which is supposed to close the gap between simulated and measured concentrations. This was found to be  $\tau = 4 \frac{1}{4}$  hours and is not directly comparable to an atmospheric suspension time or lifetime. Following sentences were also added to the manuscript: “All discrepancies between this boundary layer mixing time and a typical atmospheric lifetime are caused by assumptions which are done for eq. 7. This difference may be caused by deviations from a well-mixed constant concentration profile within the boundary layer (Figure 4), because source and removal processes in the simulation are not in equilibrium and fungal spores are continuously removed at the model boundaries.

However, using eq. 7 for calculating a potential FBAP emission flux is reasonable, because simulated fungal spore concentrations typically decrease rapidly near boundary layer height. This behavior is shown for an exemplary vertical profile in Figure 4.”

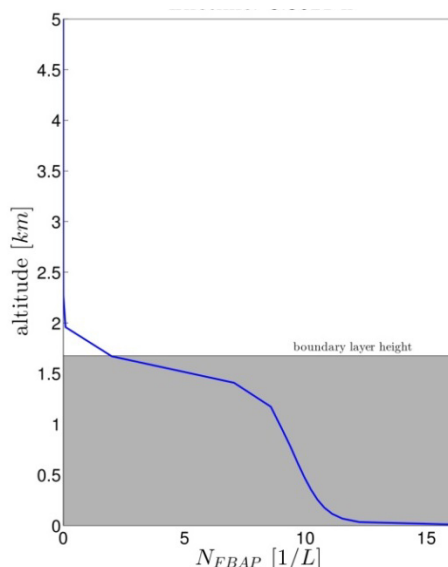


**Figure 4. Exemplary vertical profile of simulated fungal spore concentration within and above the planetary boundary layer for Karlsruhe at 28 Aug 2010 14 UTC.**

## Anonymous Referee #2

We thank the reviewer for his/her comments which have improved our manuscript. The comments are listed below in italics.

*There is insufficient statistical support for the arguments put forth in this study. The authors need to fully quantify model performance for each scheme (R=correlation coefficient and normalized mean bias statistics for Figure 3-7). In doing so, it is critical that the authors distinguish between bias and skill. Does the new scheme actually add to the model skill (i.e. improve R<sup>2</sup>) or simply eliminate bias? Are there other potential causes for the bias (i.e. LAI, qv, constants used in the model)?*

In order to improve the statistical support for this study's arguments further information on model performance is included in this reply and will be added to the manuscript. The following content to this comment is also added to the manuscript. For each time series, a correlation coefficient (R<sup>2</sup>) and a normalized mean bias (NMB; Im et al., 2013) have been calculated by

$$R^2 = 1 - \frac{\sum_{i=1}^n (M_i - \hat{O}_i)^2}{\sum_{i=1}^n (M_i - \bar{M})^2}$$

$$NMB = \frac{\sum_{i=1}^n (M_i - O_i)}{\sum_{i=1}^n O_i} 100$$

which gives an indication for a correlation between simulated fungal spore concentrations (M: N<sub>H&S</sub>, N<sub>S&D</sub>, and N<sub>FBAP</sub>) and measured FBAP concentrations (O: N<sub>F,c</sub>). Index i represents single elements of each time series. Elements calculated by a linear regression between simulated and measured concentrations are labeled with a hat, the mean value of a time series is labeled with an overbar. Results are listed in Table 1. Please note that the bottom line in Table 1 is not representing a mean value of the numbers above, but represents the result for a combination of all the time series. As noted by referee, different behaviors are found for R<sup>2</sup> and NMB and therefore it is important to distinguish between skill and bias in further discussion.

**Table 1. Correlation coefficient (R<sup>2</sup>) and normalized mean bias (NMB) for correlations between fungal spore and FBAP concentrations at different locations and three different time periods**

	N <sub>H&amp;S</sub>		N <sub>S&amp;D</sub>		N <sub>FBAP</sub>	
	R <sup>2</sup>	NMB	R <sup>2</sup>	NMB	R <sup>2</sup>	NMB
Karlsruhe, Jul10	0.0047	-57.54	0.0127	-66.30	0.0048	-31.86
Karlsruhe, Aug10	0.0125	-63.82	0.0002	20.14	0.0274	-34.68
Karlsruhe, Oct10	0.0125	-35.71	0.0052	-40.08	0.0124	1.36
Hyytiälä, Jul10	0.3268	3.18	0.3358	-67.49	0.3255	50.50
Hyytiälä, Aug10	0.0002	-57.54	0.0099	35.43	0.0511	-59.04
Hyytiälä, Oct10	0.0016	-61.74	0.0350	-75.56	0.0000	-45.97
Manchester, Aug10	0.4558	2.74	0.4274	37.72	0.4409	63.26
Killarney, Aug10	0.2408	84.42	0.0998	200.51	0.1982	213.81
<b>all</b>	<b>0.1834</b>	<b>-44.04</b>	<b>0.0551</b>	<b>-28.74</b>	<b>0.1877</b>	<b>-0.43</b>

The statistical analysis of the results indicates that NMB improves more than  $R^2$ . Differences in  $R^2$  are especially small between  $N_{H\&S}$  and  $N_{FBAP}$ , because both make use of emission rates as a function of almost the same parameters ( $N_{FBAP}$  includes an additional T-dependence). Parameters  $b_1$  and  $b_2$  (in eq. 8 of the manuscript) are estimated to give fungal spore concentrations matching best with measured FBAP concentrations. At  $T = 275.82$  K,  $F_{H\&S}$  is equal to  $F_{FBAP}$ , and temperatures above this threshold (as it is the case for almost all locations) shift  $F_{FBAP}$  to give a larger emission flux. At meteorological conditions present for the selected cases, the second part of eq. 8 dominates over the first part by a factor of  $\sim 4$  and therefore temperature changes have only a secondary influence on the emission flux. Hence,  $R^2$  is similar for both emission parameterizations.

Possible causes for the bias of  $F_{H\&S}$  and  $F_{S\&D}$  may come from different assumptions made to determine the fungal spore concentrations in ambient air. The mass size distribution of mannitol, which is used as a chemical tracer for fungal spores by Heald and Spracklen (2009), peaks in their study at particle diameters of  $\sim 5$   $\mu\text{m}$ . Additionally to fungal spores, bacteria, algae, lichens, and plant fragments, can produce mannitol and some of these can contribute to PBAP concentrations at  $\sim 5$   $\mu\text{m}$ . Similar assumptions are made for this study by linking FBAP to fungal spores, but chemical tracers vary between both studies. Furthermore, both literature-based emission fluxes compare local measurements to concentrations simulated on a global scale. Additional biases may arise when using these fluxes on a regional scale.

*The modeling in general is not very compelling and it seems like a missed opportunity to investigate/comment on the factors controlling the variability of PBAP. In particular, given the general skill of the model (e.g. Figure 3), it would be useful to try to separate in the model how meteorology and emissions contribute to variability (i.e. perform a simulation with constant emissions). This may be the first time that a model has been compared with high resolution PBAP observations. This is the primary unique direction of this work, but it is insufficiently explored in the current manuscript.*

We will expand the discussion on the relative importance of the meteorological and emission-related variability in the manuscript. A time-independent (but spatially varying) emission flux has already been included in the simulations by  $F_{S\&D}$ . Three locations consist of similar surface ecosystem properties and their emission fluxes are therefore very close to each other ( $F_{KA} = 782 \text{ m}^{-2}\text{s}^{-1}$ ;  $F_{Man} = 837 \text{ m}^{-2}\text{s}^{-1}$ ;  $F_{Kil} = 844 \text{ m}^{-2}\text{s}^{-1}$ ). The results show that diel cycles in the fungal spore concentrations also develop when using  $F_{S\&D}$  for emission. In the manuscript, the description is described as follows: "By using a time-independent (but spatially varying) emission flux  $F_{S\&D}$ , every development in the local temporal pattern arises from meteorological influences. A similar cycle develops between constant ( $F_{S\&D}$ ) and time-independent ( $F_{H\&S}$  and  $F_{FBAP}$ ) simulated fungal spore concentrations, but the order of magnitude differs to varying extend. Therefore and from by visually comparing to simulated boundary layer height, a diurnal cycle in the simulated fungal spore concentrations with a maximum between midnight and sunrise is probably influenced at least partly by boundary layer compression at night."

*1. Page 9907, lines 27-30: Regarding the role of PBAP as IN, the authors may also want to comment on the work of Hoose et al, 2010 and perhaps Creamean et al., 2013 which seem quite relevant here.*

Further comments on the role of PBAP acting as IN are now included and additional references are taken into account. The part has changed to:

“These bio-IN may be important for ice nucleation in mixed-phase clouds at temperatures warmer than  $-15^{\circ}\text{C}$  (DeMott and Prenni, 2010). In regimes colder than that, mineral dust particles and other ice nucleators are also active and the relative atmospheric abundance of PBAP is probably too small to contribute significantly to formation and evolution of these colder clouds. Previous modelling studies suggest, that bio-IN concentrations are several orders of magnitude lower than IN concentrations from mineral dust or soot and hence the influence of bio-IN on precipitation is limited on the global scale (Hoose et al., 2010; Sesartic et al., 2012; Spracklen and Heald, 2013). *In-situ* analyses of insoluble cloud ice and precipitation residuals meanwhile highlight the contribution of bio-IN to precipitation, and back trajectories indicate that they can be transported over large distances (Creamean et al., 2013).“

2. Page 9909, lines 1 and 10 seem to contradict each other, FBAP cannot be a lower limit for PBAP if it may be contaminated by other fine particles.

Uncertainties in FBAP measurements include both, a possible underestimation of PBAP as not all PBAP cause a fluorescence signal and some smaller PBAP are excluded by size selection ( $<1\ \mu\text{m}$ ), and a possible overestimation as some non-PBAP contaminate the FBAP signal to some extent. By comparison to traditional measurement techniques for PBAP, it has been found that the former aspect dominated and that FBAP can be considered a lower limit for PBAP (Pöschl et al., 2010).

3. Section 2.1: much of this is section (page 9909, line 25 through all of page 9910) is basic model treatment of aerosols that does not need to be included in a scientific manuscript. I suggest the authors trim this (equations are not necessary).

We understand the reviewer is suggestion to shorten the methodology section, but we think that a brief description of basic aerosol treatment in the model is important, especially as we are addressing readers from both the modelling and the observational communities. Descriptions of dry and wet fungal spore deposition are especially relevant for a sufficient understanding of issues about the atmospheric lifetime of fungal spores (discussed in section 3.2).

4. Page 9911, line 14: typo “gases at particulate” should be “gases and particulate”

Corrected

5. Page 9911, line 23: what are “Anthropogenic primary aerosols”?

Aerosol emissions in PM<sub>2.5</sub> and PM<sub>10</sub> size mode are disaggregated into chemical components using a split table from TNO (Kuenen et al., 2011). The category “other anthropogenic primary aerosols” represents the remaining, non-carbonaceous primary part, including e.g. minerals, metal oxides, and product emissions (Knote et al., 2011).

6. Section 2.2: line 1 and line 27 incorrectly suggest that the H&S parameterization is a constant emission rate. The authors have described how it is a dynamic function of  $q$  and LAI, therefore is by definition, not constant in time or location.

Heald and Spracklen (2009) also used a constant emission rate as a first guess and corrected it afterwards in order to give a better representation of mean mannitol concentrations, which is described in eq. 6 with a function giving  $F_{\text{H\&S}}$ . In order to not confuse the reader in future, we decided to ignore this detail and remove the citation in the first place.

7. Page 9913, line 3: Please quantitatively compare the impact of your different size assumption (3  $\mu\text{m}$ ) here with Hoose et al., 2010a (5 $\mu\text{m}$ ) and Heald and Spracklen, 2009 (PM<sub>2.5</sub>). Are your totals for mass, number emissions comparable? How did you scale your constant (c) term to account for the smaller size range from Hoose et al.?

A constant  $c = 4.6$  is applied to the number emission flux of 3  $\mu\text{m}$  particles in this study in order to have consistent mass emission flux with Hoose et al. (2010) and Heald and Spracklen (2009). The former is obtained by:

$$M_{\text{this study}} = M_{\text{Hoose 2010}} = \frac{\pi}{6} (3 \mu\text{m})^3 \rho_{\text{spore}} \underbrace{\left(\frac{5 \mu\text{m}}{3 \mu\text{m}}\right)^3}_{c=4.6} F_{\text{Hoose 2010}}$$

The latter gives a maximum fungal spore emission of  $M_{\text{H\&S}} \approx 1 \text{ g/m}^2\text{yr}$  in regions with highest LAI and  $q_v$ . For the same conditions of LAI and  $q_v$ , number emission flux from Hoose et al. (2010) gives  $F_{\text{H10}} = 500 \text{ m}^{-2}\text{s}^{-2}$ , which matches  $M_{\text{H\&S}}$  for  $\rho_{\text{spore}} = 1 \text{ g/cm}^3$  (see Figure 3a in Heald and Spracklen (2009)).

8. Page 9913, equation 6: This equation does not explicitly match the parameterization of H&S (unless one assumes that their constant= $c/(LAI_{\text{max}} q_{v_{\text{max}}})$ ). Why is the parameterization given this way here? Is there a physical justification?

We agree that the chosen formulation including an index “max” is confusing and changed it to giving the numbers directly inside the equation.

9. Page 9913, line 11: what is the time resolution for  $q_v$  (i.e. the meteorological time step)?

All meteorological parameters (including  $q_v$ ) are written out hourly. When using measured FBAP concentrations for the regression analysis, they are averaged for one hour in order to be consistent to the model output.

10. Page 9913, lines 13-18: This section is confusing. There are 3 sentences that mention the IC/BC for aerosols, and it's not clear what the authors mean by “No initial and boundary concentrations are predefined for aerosols or gases.” Please clarify or simplify this text.

Simplified in text:

“The COSMO-ART mesoscale model system is driven by initial and boundary data for meteorological conditions. They are updated every six hours and result from interpolation of the coarse grid operational atmospheric model analysis of the ECMWF (European Centre for Medium-Range Weather Forecasts).”

11. Figures 3-6: missing statistical quantification of model performance

See description above.

12. Figures 3-6: all 3 schemes co-vary. To what degree does variability reflect meteorology (PBL height, mixing, and precipitation) rather than variability in emissions driver ( $q$ , LAI)? This can be diagnosed in the simulation (statement on page 9919 lines 15-16 isn't quite true. Some of these effects can be deconvolved in the model). What is the correlation between FBAP and PBL height?

By comparing the simulated concentrations from both literature-based emission parameterizations ( $F_{S\&D} = \text{const.}$ ), influences of varying meteorological conditions and varying emission drivers are expressed. These effects cannot clearly be separated in the temporal pattern of the FBAP concentrations.

13. Page 9919, line 1: Can you show the observed precipitation from the sites in the Figures?

Exploring the correlation of FBAP concentrations to precipitation is beyond the scope of this study and is described elsewhere (e.g. Schumacher et al., 2013).

14. Page 9920, lines 7-9: Is there any evidence of this phenomenon in the observations you are exploring here?

Some of the FBAP concentrations used in this study are also included in the referenced studies (Huffman et al., 2013; Schumacher et al., 2013). An in-depth analysis of this phenomenon is beyond the scope of this study.

15. Page 9921, line 9-10: Figure 7a does not support the statement that the simulated concentrations are “systematically underestimated”. Nor does Figure 7b demonstrate the improvement suggested on page 9924, line 8. Please show statistics to support these claims.

These effects are difficult to be recognize on a log-scale, but a more detailed statistical analyses is now included.

16. Page 9922, line 3-4: what is the lifetime in the model simulations?

In the model simulation, a local estimate of the fungal spore lifetime calculated as follows:

$$\tau_{spore} = \frac{\int_{z=0}^{top} N_{spore}(z) dz}{F_{spore}}$$

The domain-average fungal spore lifetime is calculated by:

$$\tau_{spore} = \frac{\int \int \int N_{spore}(x, y, z) dx dy dz}{\int \int F_{spore}(x, y) dx dy}$$

$N_{spore}$  and  $F_{spore}$  give the fungal spore number concentration in  $1/m^3$  and emissions flux in  $1/m^2s$ , respectively, and refer to any of the three emission parameterizations. The integral runs from surface model layer (~10 m above ground) to the top-most model layer (at a height of 24 km). The atmospheric lifetime for each time period and location as temporal average are shown in Table 2.

**Table 2. Average atmospheric lifetimes of fungal spores at each location in hours.**

Hyytiälä			Karlsruhe			Killarney	Manchester
July	October	August	July	October	August	August	August
1.425	1.388	0.748	3.731	6.081	2.801	1.961	1.578

These calculations reveal a strong effect of wet deposition on the simulated lifetime, which is highest for the October case in Karlsruhe (where nearly no rain occurred in the simulation) and shortest for the August case in Hyytiälä (with extensive rain in the simulation).

17. Page 9922, line 7: *This lifetime is very short. What physical mechanism could justify such a rapid removal rate?*

As indicated in the answers to the previous comments, the model simulates a very strong wet removal of the spores. In addition, calculating the atmospheric lifetime in this simple way assumes equilibrium between local removal and source processes. At the model boundaries, fungal spores are only removed from the domain without fungal spores being transported into the domain. This disagreement may cause an underestimation of the lifetime. Sedimentation is not a major sink for fungal spores, as the average sedimentation velocity for fungal spores is  $v_{\text{sed}} = 0.035$  cm/s (calculated after Helbig et al., 2004), which is typical for 3  $\mu\text{m}$  particles.

18. Page 9923, equation 8: *Are the variables used here independent? Have you verified that you are not over-fitting?*

$q_v$  is a diagnostic variable of the model and to some extent depends on T, but an additional T-dependence has been reported for other FBAP-studies (Jones and Harrison, 2004; Di Filippo et al., 2013).

19. Figure 9: *Can you overplot the observations using the same assumptions?*

Figures 8 and 9 are modified such that an additional circle around each location gives the average measured FBAP concentration / FBAP emission flux colored with the same colorbar as the map.

## References

- Creamean, J. M., Suski, K. J., Rosenfeld, D., Cazorla, A., DeMott, P. J., Sullivan, R. C., White, A. B., Ralph, F. M., Minnis, P., Comstock, J. M., Tomlinson, J. M., and Prather, K. A.: Dust and Biological Aerosols from the Sahara and Asia Influence Precipitation in the Western U.S, *Science*, 339, 1572-1578, 10.1126/science.1227279, 2013.
- DeMott, P. J., and Prenni, A. J.: New Directions: Need for defining the numbers and sources of biological aerosols acting as ice nuclei, *Atmospheric Environment*, 44, 1944-1945, 2010.
- Di Filippo, P., Pomata, D., Riccardi, C., Buiarelli, F., and Perrino, C.: Fungal contribution to size-segregated aerosol measured through biomarkers, *Atmospheric Environment*, 64, 132-140, 10.1016/j.atmosenv.2012.10.010, 2013.
- Elbert, W., Taylor, P. E., Andreae, M. O., and Pöschl, U.: Contribution of fungi to primary biogenic aerosols in the atmosphere: wet and dry discharged spores, carbohydrates, and inorganic ions, *Atmos. Chem. Phys.*, 7, 4569-4588, 10.5194/acp-7-4569-2007, 2007.
- Gabey, A. M., Gallagher, M. W., Whitehead, J., Dorsey, J. R., Kaye, P. H., and Stanley, W. R.: Measurements and comparison of primary biological aerosol above and below a tropical forest canopy using a dual channel fluorescence spectrometer, *Atmospheric Chemistry and Physics*, 10, 4453-4466, 10.5194/acp-10-4453-2010, 2010.
- Gabey, A. M., Stanley, W. R., Gallagher, M. W., and Kaye, P. H.: The fluorescence properties of aerosol larger than 0.8  $\mu\text{m}$  in urban and tropical rainforest locations, *Atmos. Chem. Phys.*, 11, 5491-5504, 10.5194/acp-11-5491-2011, 2011.

Gabey, A. M., Vaitilingom, M., Freney, E., Boulon, J., Sellegri, K., Gallagher, M. W., Crawford, I. P., Robinson, N. H., Stanley, W. R., and Kaye, P. H.: Observations of fluorescent and biological aerosol at a high-altitude site in central France, *Atmos. Chem. Phys.*, 13, 7415-7428, 10.5194/acp-13-7415-2013, 2013.

Heald, C. L., and Spracklen, D. V.: Atmospheric budget of primary biological aerosol particles from fungal spores, *Geophys. Res. Lett.*, 36, L09806, 10.1029/2009gl037493, 2009.

Healy, D. A., Huffman, J. A., O'Connor, D. J., Pöhlker, C., Pöschl, U., and Sodeau, J. R.: Ambient measurements of biological aerosol particles near Killarney, Ireland: a comparison between real-time fluorescence and microscopy techniques, *Atmos. Chem. Phys. Discuss.*, 14, 3875-3915, 10.5194/acpd-14-3875-2014, 2014.

Helbig, N., Vogel, B., Vogel, H., and Fiedler, F.: Numerical modelling of pollen dispersion on the regional scale, *Aerobiologia*, 20, 3-19, 10.1023/b:aero.0000022984.51588.30, 2004.

Hoose, C., Kristjánsson, J. E., and Burrows, S. M.: How important is biological ice nucleation in clouds on a global scale?, *Environmental Research Letters*, 5, 024009, 2010.

Huffman, J. A., Treutlein, B., and Pöschl, U.: Fluorescent biological aerosol particle concentrations and size distributions measured with an Ultraviolet Aerodynamic Particle Sizer (UV-APS) in Central Europe, *Atmospheric Chemistry and Physics*, 10, 3215-3233, 2010.

Huffman, J. A., Prenni, A. J., DeMott, P. J., Pöhlker, C., Mason, R. H., Robinson, N. H., Fröhlich-Nowoisky, J., Tobo, Y., Després, V. R., Garcia, E., Gochis, D. J., Harris, E., Müller-Germann, I., Ruzene, C., Schmer, B., Sinha, B., Day, D. A., Andreae, M. O., Jimenez, J. L., Gallagher, M., Kreidenweis, S. M., Bertram, A. K., and Pöschl, U.: High concentrations of biological aerosol particles and ice nuclei during and after rain, *Atmos. Chem. Phys.*, 13, 6151-6164, 10.5194/acp-13-6151-2013, 2013.

Im, U., Christodoulaki, S., Violaki, K., Zampas, P., Kocak, M., Daskalakis, N., Mihalopoulos, N., and Kanakidou, M.: Atmospheric deposition of nitrogen and sulfur over southern Europe with focus on the Mediterranean and the Black Sea, *Atmospheric Environment*, 81, 660-670, <http://dx.doi.org/10.1016/j.atmosenv.2013.09.048>, 2013.

Jones, A. M., and Harrison, R. M.: The effects of meteorological factors on atmospheric bioaerosol concentrations--a review, *Science of The Total Environment*, 326, 151-180, 10.1016/j.scitotenv.2003.11.021, 2004.

Knote, C., Brunner, D., Vogel, H., Allan, J., Asmi, A., Äijälä, M., Carbone, S., van der Gon, H. D., Jimenez, J. L., Kiendler-Scharr, A., Mohr, C., Poulain, L., Prévôt, A. S. H., Swietlicki, E., and Vogel, B.: Towards an online-coupled chemistry-climate model: evaluation of trace gases and aerosols in COSMO-ART, *Geosci. Model Dev.*, 4, 1077-1102, 10.5194/gmd-4-1077-2011, 2011.

Kuenen, J., Denier van der Gon, H., Visschedijk, A., van der Brugh, H., and Gijlswijk, R.: MACC European emission inventory for the years 2003–2007, TNO, Utrecht, Netherlands, TNO-060-UT-2011-00588, 49, 2011.

Pöhlker, C., Huffman, J. A., and Pöschl, U.: Autofluorescence of atmospheric bioaerosols – fluorescent biomolecules and potential interferences, *Atmos. Meas. Tech.*, 5, 37-71, 10.5194/amt-5-37-2012, 2012.

Pöschl, U., Martin, S. T., Sinha, B., Chen, Q., Gunthe, S. S., Huffman, J. A., Borrmann, S., Farmer, D. K., Garland, R. M., Helas, G., Jimenez, J. L., King, S. M., Manzi, A., Mikhailov, E., Pauliquevis, T., Petters, M. D., Prenni, A. J., Roldin, P., Rose, D., Schneider, J., Su, H., Zorn, S. R., Artaxo, P., and Andreae, M. O.: Rainforest Aerosols as Biogenic Nuclei of Clouds and Precipitation in the Amazon, *Science*, 329, 1513-1516, 10.1126/science.1191056, 2010.

Robinson, N. H., Allan, J. D., Huffman, J. A., Kaye, P. H., Foot, V. E., and Gallagher, M.: Cluster analysis of WBS single-particle bioaerosol data, *Atmos. Meas. Tech.*, 6, 337-347, 10.5194/amt-6-337-2013, 2013.

Schumacher, C. J., Pöhlker, C., Aalto, P., Hiltunen, V., Petäjä, T., Kulmala, M., Pöschl, U., and Huffman, J. A.: Seasonal cycles of fluorescent biological aerosol particles in boreal and semi-arid forests of Finland and Colorado, *Atmos. Chem. Phys.*, 13, 11987-12001, 10.5194/acp-13-11987-2013, 2013.

Sesartic, A., Lohmann, U., and Storelvmo, T.: Bacteria in the ECHAM5-HAM global climate model, *Atmos. Chem. Phys.*, 12, 8645-8661, 10.5194/acp-12-8645-2012, 2012.

Spracklen, D. V., and Heald, C. L.: The contribution of fungal spores and bacteria to regional and global aerosol number and ice nucleation immersion freezing rates, *Atmos. Chem. Phys. Discuss.*, 13, 32459-32481, 10.5194/acpd-13-32459-2013, 2013.

Toprak, E., and Schnaiter, M.: Fluorescent biological aerosol particles measured with the Waveband Integrated Bioaerosol Sensor WIBS-4: laboratory tests combined with a one year field study, *Atmos. Chem. Phys.*, 13, 225-243, 10.5194/acp-13-225-2013, 2013.

# 1 Regional-scale Simulations of Fungal Spore Aerosols 2 Using an Emission Parameterization Adapted to Local 3 Measurements of Fluorescent Biological Aerosol Particles

4  
5  
6 M. Hummel<sup>1</sup>, C. Hoose<sup>1</sup>, M. Gallagher<sup>2</sup>, D. A. Healy<sup>3</sup>, J. A. Huffman<sup>4</sup>,  
7 D. O'Connor<sup>3</sup>, U. Pöschl<sup>5</sup>, C. Pöhlker<sup>5</sup>, N. H. Robinson<sup>2,6</sup>, M. Schnaiter<sup>1</sup>,  
8 J. R. Sodeau<sup>3</sup>, E. Toprak<sup>1</sup>, and H. Vogel<sup>1</sup>

9 [1]{Institute for Meteorology and Climate Research, Karlsruhe Institute of Technology,  
10 Karlsruhe, Germany}

11 [2]{The Centre for Atmospheric Sciences, The University of Manchester, Manchester, UK}

12 [3]{Centre for Research into Atmospheric Chemistry, Department of Chemistry, University  
13 College Cork, Cork, Ireland}

14 [4]{Department of Chemistry & Biochemistry, University of Denver, Denver, Colorado,  
15 USA}

16 [5]{Biogeochemistry Department and Multiphase Chemistry Department, Max Planck  
17 Institute for Chemistry, Mainz, Germany}

18 [\[6\]{Met Office, Exeter, UK}](#)

19 Correspondence to: M. Hummel (matthias.hummel@kit.edu)

## 21 Abstract

22 Fungal spores as a prominent type of primary biological aerosol particles (PBAP) have been  
23 incorporated into the COSMO-ART regional atmospheric model, using and comparing three  
24 different emission parameterizations. Two literature-based emission rates derived from fungal  
25 spore colony counts and chemical tracer measurements were used as a parameterization  
26 baseline for this study. A third, new emission parameterization was adapted to field  
27 measurements of fluorescent biological aerosol particles (FBAP) from four locations across  
28 Northern Europe. FBAP concentrations can be regarded as a lower estimate of total PBAP

1 concentrations. Size distributions of FBAP often show a distinct mode at approx. 3  $\mu\text{m}$ ,  
2 corresponding to a diameter range characteristic for many fungal spores. Previous studies  
3 have suggested the majority of FBAP in several locations are dominated by fungal spores.  
4 Thus, we suggest that simulated fungal spore concentrations obtained from the emission  
5 parameterizations can be compared to the sum of total FBAP concentrations. A comparison  
6 reveals that parameterized estimates of fungal spore concentrations based on literature  
7 numbers underestimate measured FBAP concentrations. In agreement with measurement data,  
8 the model results show a diurnal cycle in simulated fungal spore concentrations, which may  
9 develop partially as a consequence of a varying boundary layer height between day and night.  
10 Measured FBAP and simulated fungal spore concentrations also correlate similarly with  
11 simulated temperature and humidity. These meteorological variables, together with leaf area  
12 index, were chosen to drive the new emission parameterization discussed here. Using the new  
13 emission parameterization on a model domain covering Western Europe, fungal spores in the  
14 lowest model layer comprise a fraction of 15% of the total aerosol mass over land and reach  
15 average number concentrations of  $26 \text{ L}^{-1}$ . The results confirm that fungal spores and  
16 biological particles may account for a major fraction of supermicron aerosol particle number  
17 and mass concentration over vegetated continental regions and should thus be explicitly  
18 considered in air quality and climate studies.

19

## 20 **1. Introduction**

21 Particles emitted from biological sources are a miscellaneous and omnipresent group of the  
22 Earth's atmospheric aerosols (Elbert et al., 2007; Després et al., 2012). These primary  
23 biological aerosol particles (PBAP) can be transported over large distances and their impacts  
24 are studied by various fields of research, such as atmosphere science, agricultural research,  
25 biogeography and public health (Burrows et al., 2009). PBAP are solid airborne particles of  
26 biological origin and include microorganisms or reproductive units (e.g. bacteria, fungi,  
27 spores, pollen or viruses) as well as excretions and fragments of biological organisms (e.g.  
28 detritus, microbial fragments or leaf debris) (Després et al., 2012). Typical sizes range from  
29  $< 0.3 \mu\text{m}$  for viruses to diameters of single bacteria (0.25 - 3  $\mu\text{m}$ ), bacteria agglomerates  
30 (3 - 8  $\mu\text{m}$ ), fungal spores (1 - 30  $\mu\text{m}$ ), and up to 10 - 100  $\mu\text{m}$  for airborne pollen (Jones and  
31 Harrison, 2004; Shaffer and Lighthart, 1997; Després et al., 2012).

1 The share of atmospheric aerosol composition belonging to PBAP is large and possibly  
2 underestimated (Jaenicke et al., 2007), but is also very uncertain. Estimates of relative PBAP  
3 fraction from global models and local measurements reveal large differences between reports.  
4 On one hand, the calculated global number concentration of PBAP (zonal annual mean  
5 surface concentrations of  $10^{-2}$  -  $10^{-1}$   $\text{cm}^{-3}$ ) is below mineral dust ( $65 \text{ cm}^{-3}$ ) or soot ( $1000 \text{ cm}^{-3}$ )  
6 concentrations by several orders of magnitude (Hoose et al., 2010b). Modeling studies yielded  
7 global source strengths of  $\sim 10$  Tg/yr (plant debris and fungal spores, Winiwarter et al., 2009),  
8 56 Tg/yr (Penner, 1995), 78 Tg/yr (bacteria, fungal spores and pollen, Hoose et al., 2010a),  
9 164 Tg/yr (Mahowald et al., 2008) and 312 Tg/yr (bacteria, fungal spores and pollen,  
10 Jacobson and Streets, 2009) for different PBAP components. On the other hand,  
11 measurements of continental boundary layer air in remote vegetated regions indicate that the  
12 mass fraction of PBAP in the coarse particle size range can be as high as  $\sim 30\%$  ( $>0.2 \mu\text{m}$ ,  
13 Siberia, Matthias-Maser et al., 2000) or 65-85% ( $>1 \mu\text{m}$ , Amazonia, Martin et al., 2010;  
14 Pöschl et al., 2010; Huffman et al., 2012).

15 Like all other aerosol particles, PBAP can influence the Earth's climate by forcing the  
16 radiation budget directly (by absorbing or scattering radiation) and indirectly (by affecting  
17 cloud microphysics) (Forster et al., 2007). The direct PBAP effect on climate is difficult to  
18 estimate, because evaluations of the atmospheric PBAP concentration vary by several orders  
19 of magnitude when taking spatial and temporal divergences into account. Describing the  
20 radiative properties of PBAP is complicated, because their size ranges from fine to coarse (up  
21 to  $100 \mu\text{m}$  in diameter) and in many cases their shapes are non-spherical and not accurately  
22 known. Hence, the applicability of Mie scattering theory is limited (Després et al., 2012).  
23 However, the direct PBAP effect on global and regional climate is generally assumed to be  
24 small due to low average concentrations, in contrast to the numbers of sub-micron absorbing  
25 and scattering aerosols. The indirect PBAP effect on climate is caused by PBAP that act as  
26 cloud condensation nuclei (CCN) and/or as ice nuclei (IN). Generally, changing aerosol  
27 populations by increasing nuclei concentrations or behavior can alter the microphysical  
28 properties of clouds, thus influencing the climate system (Forster et al., 2007). Most PBAP  
29 are assumed to be good CCN, because their surface area is large compared to most other  
30 aerosol species (Petters and Kreidenweis, 2007; Ariya et al., 2009) and thus may act as so-  
31 called giant CCN (Pöschl et al., 2010). Here, the Kelvin effect can be neglected when  
32 describing water vapor condensation, and thus activation and growth proceeds quickly (Pope,  
33 2010). Some particles of biological origin (e.g. *P. syringae* bacteria and some fungal species)

1 have been found to efficiently nucleate ice growth at relatively high temperatures (Després et  
2 al., 2012; Murray et al., 2012; Hoose and Möhler, 2012; Morris et al., 2004; Morris et al.,  
3 2013; Haga et al., 2013). Biological particles have been observed ubiquitously in  
4 precipitation, fog, and snowpack (e.g. Christner et al., 2008), in clouds from airborne  
5 measurements (e.g. Prenni et al., 2009; DeLeon-Rodriguez et al., 2013) and have been shown  
6 to be important fractions of IN measured at ground level (e.g. Huffman et al., 2013; Prenni et  
7 al., 2013). These bio-IN may be important for ice nucleation in mixed-phase clouds at  
8 temperatures warmer than -15°C (DeMott and Prenni, 2010). In regimes colder than that,  
9 mineral dust particles and other ice nucleators are also active and the relative atmospheric  
10 abundance of PBAP is probably too small to contribute significantly to formation and  
11 evolution of these colder clouds. Previous modelling studies suggest, that bio-IN  
12 concentrations are several orders of magnitude lower than IN concentrations from mineral  
13 dust or soot and hence the influence of bio-IN on precipitation is limited on the global scale  
14 (Hoose et al., 2010a; Sesartic et al., 2012; Spracklen and Heald, 2013). In-situ analyses of  
15 insoluble cloud ice and precipitation residuals meanwhile highlight the contribution of bio-IN  
16 to precipitation, and back trajectories indicate that they can be transported over large distances  
17 (Creamean et al., 2013).~~These bio-IN may be important to ice nucleation in mixed-phase~~  
18 ~~clouds at temperatures warmer than -15°C (DeMott and Prenni, 2010; Hoose et al., 2010a;~~  
19 ~~Creamean et al., 2013), and therefore could influence atmospheric radiative properties on up~~  
20 ~~to regional scales. In regimes colder than that, mineral dust particles and other ice nucleators~~  
21 ~~are also active and the relative atmospheric abundance of PBAP is probably too small to~~  
22 ~~contribute significantly to formation and evolution of these colder clouds.~~

23 The methods for identifying and detecting PBAP are challenging and many different PBAP  
24 can introduce significant detection biases. Particle diameter often plays heavily into PBAP  
25 detection and characterization, and it should be noted that large discrepancies can exist  
26 between physical and aerodynamic diameter measurements (Huffman et al., 2010; Reponen et  
27 al., 2001). PBAP concentrations can be obtained either by online techniques, in which  
28 samples are analyzed by advanced instrumentation in real-time, or by offline measurement  
29 techniques. If measured offline, samples of airborne biological particles are stored under  
30 refrigeration and common methods include analysis by microscopy (stained or unmodified),  
31 by cultivation of the sample on growth media, and by amplification and detection of genetic  
32 material by sequencing or electrophoretic separation. Chemical and optical properties of  
33 PBAP samples or their tracers can be monitored in real time by: chromatography, mass

1 spectrometry, fluorescence spectrophotometry, LIDAR, and flow cytometry. Short overviews  
2 of PBAP analysis techniques have been given by Caruana et al. (2011) and Després et al.  
3 (2012).

4 This paper focuses on the mesoscale simulation of atmospheric concentrations of fungal  
5 spores. The COSMO-ART limited-area model is used for the simulations and the setup  
6 includes a model domain covering most parts of Europe with a horizontal resolution of 14 km.  
7 Two different fungal spore emission parameterizations (Heald and Spracklen, 2009; Sesartic  
8 and Dallafior, 2011) are tested by comparing their number concentrations to online laser-  
9 induced fluorescence (LIF) measurements of airborne fluorescent biological particles.  
10 Additionally, a new emission parameterization adapted to these measurements is introduced.  
11 Field data used here comes from a real-time measurement technique that detects the intrinsic  
12 (i.e. unstained) fluorescence signal, after UV excitation, of fluorophores commonly present in  
13 most biological materials (e.g. free proteins, fungal spores, bacteria, and leaf fragments).  
14 Detected particles are categorized as fluorescent biological aerosol particles (FBAP), which  
15 may broadly be considered a lower limit for the abundance of PBAP (Huffman et al., 2010;  
16 Pöhlker et al., 2012; Healy et al., 2014). FBAP were measured at four different locations  
17 (Table 1) concurrently during three focus periods in summer 2010 and fall 2010. The  
18 resulting FBAP size distribution is usually dominated by particles in the range from 2  $\mu\text{m}$  to  
19 4  $\mu\text{m}$ , which is consistent with the size of fungal spores (Huffman et al., 2010; Pöschl et al.,  
20 2010; Huffman et al., 2012; Healy et al., 2012a; Toprak and Schnaiter, 2013; Huffman et al.,  
21 2013). Further, the concentration of FBAP in a given air-mass is generally considered to  
22 underestimate PBAP concentration due to biological particles that exhibit very low levels of  
23 fluorescent emission (Huffman et al., 2012). To some extent, non-biological aerosol  
24 components can also be part of the fluorescence signal for fine particles ( $\sim 1 \mu\text{m}$ ) (Huffman et  
25 al., 2010; Toprak and Schnaiter, 2013). These factors contribute uncertainty to the  
26 parameterizations discussed here, however the overall ability of LIF techniques to provide  
27 real-time FBAP measurements allows first approximation measurements that can be  
28 enlightening.

29

## 1 2. Methodology

### 2 2.1. Model Description

3 The COSMO-ART atmospheric model system is based on the forecast model of the German  
4 weather service, combined with an online coupled module for simulating the spatial and  
5 temporal distribution of reactive gaseous and particulate components (Vogel et al., 2009).  
6 Additionally, fungal spores are incorporated as an independent, monodisperse particle class  
7 ( $d_p = 3 \mu\text{m}$ ).

8 Parameterizations for emission, sedimentation, and washout, which were originally developed  
9 for pollen dispersal, are included for this particle class (Helbig et al., 2004). Fungal spores are  
10 treated independently, as no interactions with other aerosols or gases (coagulation or  
11 condensation) are considered. The temporal development of the fungal spore number  
12 concentration is calculated by:

$$\rho \frac{d\Psi}{dt} = -\nabla \cdot \vec{F}_T - \frac{\partial}{\partial z} F_S - \lambda \Psi - \frac{1}{N} \frac{\partial}{\partial z} F_E \quad (1)$$

13 with the number mixing ratio of fungal spores being

$$\Psi = \frac{N_f}{N}, \quad (2)$$

14 and the number concentration of fungal spores  $N_f$ , the total number of particles and air  
15 molecules  $N$  per  $\text{m}^3$ , the air density  $\rho$ , the turbulent flux  $\vec{F}_T$ , the sedimentation flux  $F_S$ , a  
16 washout coefficient  $\lambda$  and a vertical emission flux  $F_E$  (Vogel et al., 2008). The turbulent flux  
17 is calculated by  $\vec{F}_T = \overline{\rho v' \Psi'}$ , incorporating the turbulent fluctuations of wind speed  $v'$  and  
18 fungal spore number mixing ratio  $\Psi'$ . Fungal spore sedimentation is calculated  
19 by  $F_S = \rho \Psi v_s$ . The fungal spore settling velocity  $v_s$  is calculated by applying the volume-  
20 equivalent particle diameter  $d_e = 2 \sqrt[3]{a^2 b}$ , with  $a = 2.1 \mu\text{m}$  and  $b = 5 \mu\text{m}$  (Yamamoto et al.,  
21 2012) being the major and minor radius of a prolate spheroid. This results in:

$$v_s^2 = \frac{4 \rho_p d_e g}{3 \rho c_d} \quad (3)$$

22 where  $\rho_p = 1 \text{ g/cm}^3$  is the spore density (Trail et al., 2005; Gregory, 1961) and  $c_d$  the drag  
23 coefficient (Aylor, 2002). The calculation of the washout coefficient is based on the  
24 assumption of raindrops being much larger than aerosol particles and having a much higher  
25 terminal fall velocity. It yields:

$$\lambda(d_p) = \int_0^{\infty} \frac{\pi}{4} D_D^2 v_t(D_D) E(d_p, D_D) n(D_D) dD_D \quad (4)$$

1 (Rinke, 2008).  $D_D$  and  $d_p$  are the diameters of raindrops and particles, respectively,  $v_t(D_D)$  is  
 2 the terminal fall velocity,  $E$  is a collision efficiency and  $n(D_D)$  is the size distribution of the  
 3 raindrop number concentration. For fungal spores with a spherical diameter of 3  $\mu\text{m}$ , the  
 4 collision efficiency  $E$  with 0.1 mm and 1 mm droplets is approximately 0.085 and 0.3,  
 5 respectively.

6 Adapting the model for simulations of fungal spores requires inclusion of an emission flux  $F_E$   
 7 in the source term of eq. (1) by means of an emission parameterization which will be  
 8 described in the next section.

9 Together with fungal spore simulations COSMO-ART is used to compute the mass  
 10 concentration of major atmospheric aerosol components. Hence, the proportion of fungal  
 11 spores with respect to the dry aerosol mass can be estimated (section 3.4). In addition to  
 12 primary aerosol emissions, further gaseous emissions given by the EMPA emission dataset  
 13 (section 2.3) are taken into account. Partitioning of inorganic aerosol components between the  
 14 gases at-and particulate phase is simulated by the ISORROPIA II module (Fountoukis and  
 15 Nenes, 2007). Condensation on fungal spore aerosols is not included. The contribution of  
 16 secondary organic aerosols (SOA) to the particles is handled by condensation of oxidized  
 17 volatile organic compounds as described by Schell et al. (2001). When soot aerosols are not  
 18 involved as a solid nuclei enabling condensation, clusters build by gas-to-particle conversion  
 19 via binary nucleation of sulfuric acid and water. They are computed as an individual particle  
 20 mode. All aerosol particles including these chemical compounds are assumed to be internally  
 21 mixed. A soot mode without mixing of other chemical compounds is included as particles that  
 22 are emitted directly into the atmosphere. Anthropogenic primary aerosols (aPA) in the coarse  
 23 size range ( $<10 \mu\text{m}$ ) are treated as a separate mode. Detailed descriptions are given in Vogel  
 24 et al. (2009). Furthermore, sea salt is included in the model simulation and its emission is  
 25 related to sea water temperature and wind speed (Lundgren et al., 2013). No desert dust  
 26 emissions are included, as the model domain does not cover the corresponding emission  
 27 regions and no transport into the model domain is taken into account.

28

## 2.2. Emission Parameterization of Fungal Spores

In literature, a constant emission rate was used as input of a global chemical transport model to represent the magnitude and range of measured concentrations of mannitol as a molecular tracer for basidiospores (Elbert et al., 2007). Broad geographical differences can be included in the emission flux by distinguishing between ecosystems. While reviewing the measured data available on measured fungal spore concentrations, Sesartic and Dallafior (2011) calculated number fluxes of fungal spore emissions for six different ecosystems (defined by Olson et al., 2001). Four of these emission fluxes were included into COSMO-ART, and coupled to ecosystem definitions by the GLC2000 (Global Landcover 2000 Database) (forest and shrubs) and Ramankutty et al. (2008) (grassland and crops). The sum of these fluxes, as defined by Sesartic and Dallafior (2011), are emitted from the land area fraction  $E_i$  of each ecosystem  $i$  ( $\sum_i^n E_i = 1$  for  $n$  number of ecosystems), gives the total emission flux  $F_E = F_{S\&D}$  in  $\text{m}^{-2}\text{s}^{-1}$  of eq. (1) for fungal spores:

$$F_{S\&D} = 214 \text{ m}^{-2}\text{s}^{-1} E_{forest} + 1203 \text{ m}^{-2}\text{s}^{-1} E_{shrub} + 165 \text{ m}^{-2}\text{s}^{-1} E_{grassland} + 2509 \text{ m}^{-2}\text{s}^{-1} E_{crop} \quad (5)$$

Additionally, a second emission parameterization was tested, which varies as a function of meteorological and surface conditions. Jones and Harrison (2004) reviewed the relations determined when analyzing the observed fungal spore concentrations and atmospheric factors. Seasonal variations can be explained by changes in the leaf area index ( $LAI$ ). This was verified by correlation to the observed mannitol concentrations. Among the drivers of day-to-day variations, specific humidity ( $q_v$ ) correlates best with the mannitol concentrations (Heald and Spracklen, 2009). It was argued that though other atmospheric factors (e.g. temperature) may actually drive the correlation, this does not change correlation results and thus parameterizations can proceed without having information about the root drivers of fungal spore release. ~~A constant~~The emission rate ~~was used here by~~ is linearly scaled ~~ing with~~  $LAI$  and  $q_v$  in order to give global fungal spore concentrations matching the mean mannitol concentrations (Heald and Spracklen, 2009). In order to fit to the emission flux specified in Hoose et al. (2010a) for a spore diameter of  $5 \mu\text{m}$ , a constant  $c$  is set to  $c = 2315 \text{ m}^{-2} \text{ s}^{-1}$  to be appropriate for fungal spores with  $3 \mu\text{m}$  in diameter. Based on the emission flux in eq. (1), this gives an alternative source  $F_E = F_{H\&S}$  of fungal spores in  $\text{m}^{-2}\text{s}^{-1}$ :

$$F_{H\&S} = c \frac{LAI}{5 \text{ m m}^{-2}} \frac{q_v}{1.5 \times 10^{-2} \text{ kg kg}^{-1}} \quad (6)$$

1 *LAI* is the leaf area index,  $q_v$  is the specific humidity at the surface, ~~and their scaling factors~~  
 2 ~~adapted from tropical rain forest conditions are assumed to be  $LAI_{max} = 5 \text{ m}^2 \text{ m}^{-2}$  and~~  
 3  ~~$q_{v,max} = 1.5 \times 10^{-2} \text{ kg kg}^{-1}$ .~~ In the COSMO-ART simulations *LAI* is horizontally distributed  
 4 according to GLC2000 containing monthly variation and  $q_v$  is provided by the model as a  
 5 meteorological variable.

### 7 **2.3. Model Domain and Input Data**

8 The COSMO-ART mesoscale model system is driven by initial and boundary data for  
 9 meteorological ~~and aerosol and chemistry~~ conditions. ~~The meteorological conditions~~ They are  
 10 updated every six hours and result from interpolation of the coarse grid operational  
 11 atmospheric model analysis of the ECMWF (European Centre for Medium-Range Weather  
 12 Forecasts). No initial and boundary concentrations are predefined for aerosols or gases.  
 13 Therefore, all gaseous species are set to a climatological, homogeneously distributed initial  
 14 concentration. ~~The and~~ emission rates for chemical compounds included in the ART part are  
 15 updated hourly. They are provided by EMPA (Swiss Federal Laboratories for Materials  
 16 Science and Technology) based on the TNO/MACC (Monitoring Atmospheric Composition  
 17 and Climate) inventory (Kuenen et al., 2011). The treatment of emissions for COSMO-ART  
 18 can be found in Knote et al. (2011). Homogeneously distributed mass densities for each  
 19 aerosol are used as initial conditions, together with the aerosol size distribution and particle  
 20 density. Primary particle emissions are included as parameterizations based on meteorological  
 21 and surface conditions. Land use data and constant surface properties are derived from the  
 22 GLC2000 database (Bartholomé and Belward, 2005). All parameters are post-processed to the  
 23 rotated spherical coordinate system of COSMO-ART (Doms and Schättler, 2002). For the  
 24 purpose of this paper, the model domain covers most parts of Western Europe from mainland  
 25 Portugal to northern Finland, the longitudinal extension being 2849 km the latitudinal  
 26 extension being 3803 km with a horizontal spacing of  $0.125^\circ$  ( $\cong 14 \text{ km}$ ) on a rotated grid. In  
 27 vertical direction the model reaches up to an altitude of about 24 km distributed over 40  
 28 terrain-following levels. The time stepping of the Runge-Kutta dynamical core is set to 30 s.

## 1 2.4. Auto-fluorescence Measurements

2 Ambient aerosols can be roughly classified as biological or not by interrogating particles at  
3 characteristic wavelengths of excitation and measuring the resultant emission in a process  
4 called ultraviolet light-induced fluorescence (UV-LIF) (e.g. Hairston et al., 1997; Pan et al.,  
5 1999). In particular, the region of fluorescent excitation near 360 nm is often used as  
6 characteristic of certain cell metabolites present in all living cells, including riboflavin and  
7 reduced pyridine nucleotides (e.g. NAD(P)H). The region of excitation near 270 nm includes  
8 certain amino acids (e.g. tryptophan) contained in ~~all~~most proteins. However, many other  
9 biological fluorophores exist and the relationship between the measured fluorescence of  
10 complex biological particles and fluorophore assignment is very complex (Pöhlker et al.,  
11 2012; Pöhlker et al., 2013).

12 Two instrument types were utilized at four locations for the comparison discussed in this  
13 paper. The ultraviolet aerodynamic particle sizer (UV-APS; TSI, Inc., Shoreview, MN, USA)  
14 measures particle size aerodynamically, excites individual particles using a single Nd:YAG  
15 laser pulse at 355 nm, and detects integrated fluorescent emission (non-dispersed) in a single  
16 wavelength region between 420 nm and 575 nm (Hairston et al., 1997; Brosseau et al., 2000;  
17 Huffman et al., 2010). The Waveband Integrated Bioaerosol Sensor (WIBS, versions 3 and 4;  
18 University of Hertfordshire, UK) measures particle size optically and excites individual  
19 particles via two sequential pulses from a Xe-flash lamp, at 280 nm and 370 nm, respectively  
20 (e.g. Kaye et al., 2005; Foot et al., 2008). Fluorescence for each particle is then measured in  
21 one of two wavelength regions, resulting in three measured fluorescence parameters for each  
22 WIBS instrument named FL1\_280, FL2\_280, and FL3\_370. See Gabey et al. (2010) and  
23 Robinson et al. (2013) for more details, including slight differences in WIBS-3 and WIBS-4  
24 models. The number concentration of FBAP can be written as  $N_{F,c}$  with subscripts referring to  
25 fluorescent and coarse particle size. The differences in the pairs of wavelengths used for  
26 fluorescence, as well as the possible differences in sensitivity between instruments, suggest  
27 that the term “FBAP” as determined by each instrument is not rigorously interchangeable, and  
28 it is critical to understand the method of analysis when comparing datasets. For example, the  
29 ambient FBAP number concentration as determined by UV-APS has been shown to be  
30 qualitatively consistent with the number concentration of particles that fluorescence in the  
31 WIBS FL3\_370 channel, while the  $N_{F,c}$  comparison between UV-APS and WIBS FL1\_280  
32 channel is relatively poor (Healy et al., 2014). Here we use the term FBAP from WIBS data to

1 mean particles that exhibit fluorescence simultaneously in both channels FL1\_280 and  
2 FL3\_370.

3 Particle size can aide differentiation between biological particles classes observed, however  
4 the selectivity based on size alone is very uncertain. For example, and to a rough first  
5 approximation, it may be true that many FBAP  $\sim 1 \mu\text{m}$  are single bacterial particles and that  
6 many FBAP 2 - 6  $\mu\text{m}$  may be fungal spores or bacterial agglomerates (Shaffer and Lighthart,  
7 1997). However, biological species can vary widely, and other FBAP classes (e.g. fragments  
8 of larger PBAP, internal components of burst pollen, the presence of other biological species)  
9 confound the simple assignment of FBAP based on size (Després et al., 2012).

10 Further, at least a fraction of fluorescent, supermicron particles are likely to come from non-  
11 biological sources, and thus could be counted as FBAP. These non-biological process include  
12 anthropogenic sources (e.g. polycyclic aromatic hydrocarbon particles from combustion and  
13 cigarette smoke), present most often in submicron particles (Huffman et al., 2010), select  
14 oxidized organic aerosol particles (e.g. absorbing brown carbon particles) (Bones et al., 2010;  
15 Lee et al., 2013), and some humic-like substances (Gabey et al., 2013). For example, at the  
16 rural, elevated site of Puy de Dôme, France, WIBS-3 FBAP measurements were compared to  
17 results from fluorescence microscopy paired with staining of fungal spores and bacteria.  
18 These results suggest that the real-time UV-LIF measurements indeed track the diurnal cycle  
19 of the bacteria concentration, but that non-biological particles still contributed significantly to  
20 fluorescent particle number (Gabey et al., 2013).

21 Virtually every ambient measurement study performed with the WIBS or UV-APS to date has  
22 shown a dominant FBAP mode peaking at 2 - 4  $\mu\text{m}$  in size (Huffman et al., 2010; Huffman et  
23 al., 2012; Huffman et al., 2013; Gabey et al., 2010; Toprak and Schnaiter, 2013; Healy et al.,  
24 2014). For example, the FBAP size distributions measured at each of the four sampling  
25 locations discussed here is shown in Figure 1, highlighting the common presence of the  
26 2 - 4  $\mu\text{m}$  peak. It has been proposed that fungal spores and bacteria agglomerates are the most  
27 dominant biological aerosols in this size range (Jones and Harrison, 2004; Després et al.,  
28 2012; Fang et al., 2008) and that the FBAP signal in this size range is typically dominated by  
29 fungal spores. This was corroborated in more detail for a remote Amazonian site using FBAP  
30 analysis along with fluorescence microscopy of stained filter samples (Huffman et al., 2012),  
31 but has not yet been rigorously tested in other environments. [At the costal site of Killarney,](#)  
32 [results of fluorescence and optical microscopy of impacted biological particles reveal that](#)

1 | some PBAP, e.g. Spores of *Cladosporium spp.*, which have been frequently observed in many  
2 | environments, were not correlated to the FBAP concentration (Healy et al., 2014). However,  
3 | particle size modes of WIBS channel FL2 280 correlate with the concentration of airborne  
4 | fungal spores commonly observed at the sampling site (Healy et al., 2014). Other microscopy  
5 | and DNA-based studies have suggested that fungal spores constitute the largest fraction of  
6 | PBAP in the 2 – 4 µm size (e.g. Graham et al., 2003; Lin and Li, 1996; Burch and Levetin,  
7 | 2002). Bauer et al. (2008) showed that fungal spores account for an average of 60% of the  
8 | organic content in the particulate matter in a size range of 2 - 10 µm in rural and urban areas  
9 | of Vienna, Austria.  
10

### 1 3. Results

#### 2 3.1. Comparison of Time Series of Measured FBAP and Simulated Fungal 3 Spores

4 Fungal spore concentrations simulated using the emission flux given in eqs. (5) and (6)  
5 according to Heald and Spracklen (2009) and Sesartic and Dallafior (2011) were first  
6 compared to FBAP measurements without further adjustment. An overview of time series for  
7 all measurements and simulations discussed here is shown in Figure 2 by a box-and-whiskers  
8 plot. Time periods for each of three case studies (Table 1) were chosen as exemplary periods  
9 when UV-LIF instruments were operating simultaneously at a minimum of two locations,  
10 with no requirements applied with respect to environmental conditions. For the statistical  
11 analysis, FBAP measurements were averaged over one hour periods in order to be consistent  
12 to the model output time steps. For most time periods at Karlsruhe and Hyytiälä the simulated  
13 fungal spore concentrations are smaller than the measured FBAP concentrations (Figure 2).  
14 This difference is highest at Hyytiälä in August 2010. At Hyytiälä in July and at Manchester  
15 and Killarney in August, the Heald and Spracklen (2009) emission ( $F_{H\&S}$ ) gives median  
16 concentration values which agree reasonably well with the measurements. During October,  
17 the fungal spores number concentrations based on constant emission fluxes given by Sesartic  
18 and Dallafior (2011) ( $F_{S\&D}$ ) agree best with the measured FBAP concentrations. Long-term  
19 analysis of FBAP measurements, including periods at the Karlsruhe (Toprak and Schnaiter,  
20 2013) and Hyytiälä site (Schumacher et al., 2013) discussed here, shows an annual cycle of  
21 average FBAP number concentrations peaking in summer and lowest in winter. Thus, a  
22 simulation based on a constant emission flux may not be appropriate to reproduce the FBAP  
23 concentrations.

24 Figures 3 to 6 show a series of one-week long case studies, each representing two  
25 measurement sites. The plots show comparisons between simulation and measurement time  
26 series for each station. The simulated fungal spore number concentration is given for the  
27 model grid point closest to the measuring site. Due to model spin-up, the first six hours of the  
28 simulated fungal spore concentrations are removed from the figures and are not included in  
29 the analysis. The total precipitation calculated by the model is shown by gray bars with the  
30 ordinate on the right hand side of the figure. The simulated boundary layer height is also  
31 included at the bottom of each panel in the figures.

1 Measured FBAP number concentrations often exhibit distinct diel (24-h) cycles with a  
2 maximum in the morning hours or around midnight and a minimum around noon. These  
3 features have been consistently reported by most studies discussing temporal behavior of  
4 FBAP (Gabey et al., 2010; Huffman et al., 2010; Huffman et al., 2012; Toprak and Schnaiter,  
5 2013). Here, a similar diel cycle is frequently obtained from simulations, and the simulated  
6 fungal spore concentrations often anti-correlate with the simulated boundary layer height  
7 ( $h_{PBL}$ ) (Figures 3 to 6). The measured FBAP concentrations often qualitatively track the  
8 general pattern of simulated  $h_{PBL}$ , however the magnitude of concentration change and the  
9 timing is often not consistent. For example, on 24 and 25 July at the Karlsruhe site (Figure 3a)  
10 a boundary layer compression during the night leads to an increase in the simulated fungal  
11 spore concentrations by a factor of  $\sim 4$ , and during day the concentrations decreases as the  
12 boundary layer rises again. In this case, the measured FBAP concentrations are in relatively  
13 good agreement with the simulated fungal spore numbers, with  $N_{F,c}$  dropping slowly during  
14 the day on 24 and 27 July, and to a rate closer to the simulations on 25 July. This suggests that  
15 FBAP concentrations were likely influenced, at least partially, by the changing boundary  
16 layer height, though diel changes in biological emission are also likely to influence diel FBAP  
17 patterns. A similar temporal pattern in simulated fungal spore concentrations is shown in  
18 Figure 4a, where a maximum in  $h_{PBL}$  at 12 and 13 October occurs approximately coincident  
19 with a minimum in the simulated number concentration. In this case, however, the measured  
20 FBAP concentrations do not reflect the diel pattern of the simulations. On 31 August (Figure  
21 5a), measured FBAP and simulated fungal spore number concentration increase  
22 simultaneously and parallel to the boundary layer compression, but the increase is more  
23 intense for FBAP measurements than for spore simulations. Additionally, at Manchester  
24 between 31 August and 1 September (Figure 6a) measured and simulated concentrations are  
25 in good agreement. Distinct minima and maxima clearly anti-correlate with the minima and  
26 maxima of the boundary layer height. In contrast, during the same time period in Killarney  
27 (Figure 6b), small changes in the boundary layer were simulated along with minor changes in  
28 fungal spore concentrations. In this case, measured FBAP concentrations qualitatively reflect  
29 the same temporal pattern of number concentration, but show poor trend consistency with  
30  $h_{PBL}$ . The magnitude of diel FBAP concentration change was similar throughout the week  
31 shown, whereas  $h_{PBL}$  showed large diel variations between 26 and 30 August and relatively no  
32 change in  $h_{PBL}$  from 30 August to 1 September. Figures 3b, 4b, and 5b also show diel FBAP  
33 concentration changes that correlate poorly with simulated  $h_{PBL}$ . We conclude that (i)

1 simulated fungal spore concentrations are sensitive to changes in the simulated boundary  
2 layer height, by extension, that (ii) diel cycles of FBAP concentrations are likely to be  
3 partially influenced by diel cycles of boundary layer height, but that (iii) the development of  
4 the FBAP concentration is in addition influenced by daily cycles in biological emission  
5 processes, including those of fungal spores and other PBAP classes. These competing effects  
6 are impossible to separate by this analysis.

7 A comparison of measured FBAP and simulated fungal spore number concentrations for July  
8 2010 is shown in Figure 3. At the measurement site of Karlsruhe, diel cycles were found in  
9 the simulated and measured time series, with constantly lower concentrations being obtained  
10 from simulations based on emission parameterizations given in literature. When precipitation  
11 occurs in the simulation, the simulated fungal spore concentrations decrease due to washout  
12 and the diel development of the concentration is interrupted. Afterwards, the simulated  
13 concentrations quickly return to the previous baseline. At Hyytiälä a strong decrease in  
14 simulated fungal spore concentration on 24 July precisely overlaps with the simulation of  
15 precipitation. After hitting a minimum value during simulated precipitation, the simulated  
16 fungal spore concentration increases steadily for two days as a result of a post-frontal shift in  
17 wind direction and decrease in wind speed. The increase is also reflected in the measured  
18 FBAP concentrations. However, the simulated precipitation values do not always coincide  
19 with precipitation at the site, as was the case in this instance. As a result of no rain falling at  
20 the site on 24 July, the measured FBAP concentration was not affected by the simulated rain.  
21 While this example shows that uncertainty in local meteorology contributes uncertainty to the  
22 aerosol output of the model, washout from precipitation remains an important modeled  
23 process for estimating FBAP concentrations. Additionally, other dynamic processes are  
24 known to affect FBAP concentrations. For example, FBAP has been shown to increase  
25 dramatically during rainfall, a process reported recently for both a site in Colorado (Huffman  
26 et al., 2013) and also at the Hyytiälä site (Schumacher et al., 2013). The reasons for this  
27 FBAP increase are unclear, but are thought to be related to mechanical ejection from  
28 terrestrial surfaces as a result of rain droplet splash (Huffman et al., 2013). These effects are  
29 known to be dependent on the local geography and ecology, however, and are outside the  
30 scope of the presented emission parameterizations.

31 During the simulation period of October 2010, the simulated fungal spore number  
32 concentrations  $F_{H\&S}$  are consistently below the measured FBAP concentrations at the sites of

1 Karlsruhe and Hyytiälä, whereas  $F_{S\&D}$  matches the relative magnitude of the measurements  
2 more closely in both cases (Figure 4). At Karlsruhe, concentrations simulated by each  
3 emission parameterization follow a distinct diel cycle and increase slightly through the week,  
4 reaching concentration maxima on 15 October. The measured FBAP concentration develops  
5 differently, with only very weak diel cycle present from 11 to 14 October, and showing little  
6 relationship to the simulated  $h_{PBL}$ , as discussed above.

7 At the end of August 2010, four different measurement series were available for a comparison  
8 to fungal spore simulations (Figure 5 and 6). The measured time series of FBAP number  
9 concentrations generally exhibit diel cycles, as discussed. The absolute FBAP concentration  
10 at Hyytiälä was consistently highest, when comparing all four sites. This trend is even more  
11 obvious when comparing the median concentrations on a linear scale (Figure 2). As a result,  
12 concentrations simulated from the literature-based parameterizations under-predict  
13 measurements by the greatest margin at Hyytiälä. This under-prediction is likely a result of  
14 the persistent precipitation simulated by the model and is an indication that precipitation has a  
15 stronger influence on the simulated concentrations than changes in the boundary layer height.  
16 Measured rainfall during this period at Hyytiälä was less consistent than the model predicts,  
17 but occurred with episodic peaks. In all other August case studies, simulated fungal spore  
18 concentrations show relatively good agreement with FBAP measurements.

19

### 20 **3.2. Development of a Fungal Spore Emission Parameterization by Adaptation** 21 **to FBAP Measurements**

22 Direct comparison between simulated fungal spores and measured FBAP reveals that in  
23 general the simulated concentrations systematically underestimate the measured  
24 concentrations (Figure 8a). This difference is most distinct at Hyytiälä during the August case  
25 study and at Karlsruhe in the July and October case study. Here we suggest an improved  
26 parameterization, including meteorological and surface parameters identified earlier as drivers  
27 of fungal spore emissions. Additionally, new parameters driving fungal spore emissions have  
28 been investigated. The emission flux depends on these parameters and their fitting  
29 coefficients obtained from a regression analysis of the FBAP measurements. The new  
30 parameterization for fungal spore emissions has been incorporated into COSMO-ART and the  
31 resulting concentrations are included in Figures 3 to 6.

1 The emission flux from the regression analysis is adjusted to an emission flux  $F_{F,c}$  estimated  
2 from the FBAP number concentration. For this, it is assumed that particles are evenly  
3 distributed throughout the planetary boundary layer and that the simulated fungal spore  
4 concentration negatively correlates with  $h_{PBL}$ . Together with a steady-state condition and  
5 neglecting horizontal exchanges with the surrounding air, the balance holds between the  
6 number concentration ( $N_f$ ) and the emission rate ( $F_{F,c}$ ) together with the atmospheric lifetime  
7 of fungal spores ( $\tau$ ):

$$N_f = \frac{F_{F,c} \tau}{h_{PBL}} \quad (7)$$

8 (Seinfeld and Pandis, 2006). The boundary layer height at the measurement site needs to be  
9 taken from the model simulation as it is not measured consistently. Here,  $\tau$  the fungal spore  
10 lifetime represents a boundary layer mixing time and is not identical to an atmospheric  
11 residence time. For an initial test simulation,  $\tau$  is assumed to be constant and is estimated with  
12 an initial value of one day, as given in literature for atmospheric lifetimes of aerosol particles  
13 with 3  $\mu\text{m}$  in diameter (Jaenicke, 1978). ~~A new simulation of~~ In this case, the fungal spore  
14 concentrations with the initial value of atmospheric spore lifetime reveals an underestimation  
15 compared to the FBAP measurements. As a remedy, the ~~fungal spore lifetime  $\tau$~~  is corrected to  
16  $\tau = 4 \frac{3}{4}$  hours which can be understood as a mean time for boundary layer mixing of fungal  
17 spores. The deviation from a lifetime of 3  $\mu\text{m}$  particles given in literature may be attributed to  
18 the assumption of a constant vertical distribution of fungal spores with increasing altitude  
19 until boundary layer height. However, a ratio of approximately 1.75 between surface-level  
20 concentrations and mean concentrations within the boundary layer is too small to explain the  
21 discrepancy and fungal spores above boundary layer may stay in atmosphere for longer  
22 times in lifetime. All discrepancies between this boundary layer mixing time and a typical  
23 atmospheric lifetime are caused by assumptions which are done for eq. (7). This difference  
24 may be caused by deviations from a well-mixed constant concentration profile within the  
25 boundary layer, because source and removal processes in the simulation are not in equilibrium  
26 and fungal spores are continuously removed at the model boundaries. However, using eq. (7)  
27 for calculating a potential FBAP emission flux is reasonable, because simulated fungal spore  
28 concentrations typically decrease rapidly near boundary layer height. This behavior is shown  
29 for an exemplary vertical profile in Figure 7.

30

1

2 Two types of instruments operating with different numbers of channels and detecting  
3 fluorescence at different wavelengths are used here for deriving an emission parameterization  
4 appropriate for fungal spores. The technical difference may lead to slightly deviating FBAP  
5 concentrations (Healy et al., 2014), because the WIBS instrument only counts particles as  
6 FBAP when a signal exceeds a threshold in both channels (Pöhlker et al., 2012; Gabey et al.,  
7 2010). Some fungal spores most abundant in the Earth's atmosphere and very common for  
8 fungal spores of 2 - 4  $\mu\text{m}$  (*Cladosporium sp.*, *Aspergillus versicolor*, *Penicillium solitum*)  
9 (Fröhlich-Nowoisky et al., 2012; Hameed and Khodr, 2001) only show a weak signal in the  
10 emission wavelength of 310 nm to 400 nm (Saari et al., 2013; Healy et al., 2014). This  
11 difference needs to be taken into account when comparing absolute concentrations of fungal  
12 spores and FBAP. During the time periods shown here, the WIBS indicate slightly lower  
13 FBAP concentrations than the UV-APS when comparing to the model results. In general, this  
14 feature is not always valid and detailed side-by-side comparisons between the two types of  
15 instruments are required to determine their behavior in terms of FBAP detection and  
16 estimation of the PBAP concentration. In the attempt to factor out the technical difference  
17 between the instruments, we assume that FBAP concentration can be multiplied by a constant  
18 factor for the concentration values to match each other. The amount of FBAP given by the  
19 UV-APS may be represented best by WIBS channel FL3\_370 (section 2.4). The FBAP  
20 concentration given by the UV-APS is therefore reduced by a factor derived from the WIBS  
21 instrument as the mean ratio between channel FL3\_370 and the total FBAP concentration  $N_{F,c}$   
22 (channels FL1\_280 and FL3\_370). The factor is estimated to be 2.2 and identical for WIBS  
23 data at Karlsruhe and Manchester. The difference is not taken into account in the comparison  
24 of the time series in section 3.1, but corrected before applying eq. (7).

25 Analyzing the meteorological and surface parameters of the model output, it was found that a  
26 better correlation with the measured FBAP concentrations is achieved for specific humidity  
27 rather than relative humidity, as it was reported for previous field measurements (Gabey et al.,  
28 2010; Toprak and Schnaiter, 2013; Di Filippo et al., 2013). During the time period in July  
29 2010, the measured FBAP concentrations vary in a narrow range of specific humidity, which  
30 is not reproduced by the literature-based simulation. For this reason, the July case study was  
31 removed from the regression analysis. A dependence on the *LAI* is required in order to take  
32 the seasonal change into account and to distinguish among various regions. A combination of

1 *LAI* and specific humidity in the regression has the advantage of reducing the fitting  
 2 parameters. The same relation was chosen by Heald and Spracklen (2009) for the previously  
 3 discussed emission parameterization. Additionally, surface temperature dependence as  
 4 suggested by Di Filippo et al. (2013) is indicated by the time series and factored in a  
 5 regression analysis. The parameters ( $b_1 = 20.426$  and  $b_2 = 3.93 \times 10^4$ ) are estimated to be the  
 6 smallest sum of all squared residuals and result in a multiple linear regression giving an  
 7 emission flux  $F_E = F_{FBAP}$  in  $\text{m}^{-2}\text{s}^{-1}$  for fungal spores fitted to FBAP measurements:

$$F_{FBAP} = b_1 (T - 275.82 \text{ K}) + b_2 q_v LAI \quad (8)$$

8 where  $T$  is the surface temperature in K,  $q_v$  the specific humidity in  $\text{kg kg}^{-1}$ , and  $LAI$  the leaf  
 9 area index in  $\text{m}^2 \text{m}^{-2}$ . The parameter inside the parentheses is related to an emission offset of  
 10 the regression and covers unknown influences. The coefficient  $b_2$  is approximately the same  
 11 as the constants in the Heald and Spracklen (2009) emission for a particle diameter of  $3 \mu\text{m}$   
 12 given in eq. (6). The additional temperature dependence in eq. (8) increases the fungal spore  
 13 emission for temperatures above 275.8 K and lowers the emission for temperatures below this  
 14 value.

15 The multiple linear regression yields a coefficient of determination of  $R^2 = 0.4$ . By comparing  
 16 the simulated concentrations (based on  $F_{FBAP}$ ) to the measured FBAP concentrations, it is  
 17 found that they distribute more evenly along the 1:1 line (Figure 8b). The statistical overview  
 18 (Figure 2) shows a better agreement between the median concentrations of simulation and  
 19 measurement for the new emission parameterization than for the literature-based emissions,  
 20 which is most obvious at Karlsruhe in August and at Hyytiälä in July. The new emission  
 21 parameterization only slightly reduces the underestimations found for Hyytiälä during  
 22 August.

23 Figure 9 shows the emission flux for late August 2010, following the new parameterization,  
 24 horizontally distributed over a model domain covering Europe. Here, averaged over land  
 25 areas of the domain,  $F_{FBAP}$  gives  $1.03 \times 10^3 \text{ m}^{-2}\text{s}^{-1}$ . During July and October, the average flux  
 26 is shifted to  $1.4 \times 10^3 \text{ m}^{-2}\text{s}^{-1}$  and  $0.4 \times 10^3 \text{ m}^{-2}\text{s}^{-1}$ , respectively, mainly as a result of seasonal  
 27 changes of  $LAI$  and  $T$ .

28 When analyzing the temporal development of the simulated fungal spore concentrations for  
 29 each time series,  $F_{FBAP}$  mostly results in a slightly higher number concentration than  $F_{H\&S}$  or  
 30  $F_{S\&D}$  (Figures 3 to 6). This is not the case for October 2010, where the  $F_{FBAP}$ -concentrations

1 are in the range of the literature-based concentrations. A sharp decrease on 15 October at  
2 Hyytiälä, which is not reflected by the literature-based simulation, is caused by a rapid  
3 temperature change. Comparison for the August case study show that simulated  $F_{FBAP}$ -  
4 concentrations agree well with measured FBAP concentrations without overestimating the  
5 measurement at Manchester and Killarney, where literature-based simulations and  
6 measurements already correspond to each other. Only a slight overestimation can be found at  
7 Manchester, which might be due to an urban measuring site that is not represented accurately  
8 by the model setup with its broad resolution.

### 9 10 3.3. Statistical Correlation between Measured FBAP and Simulated Fungal 11 Spore Concentration

12 The statistical analysis of the results indicates that normalized mean bias NMB improves  
13 more than the correlation coefficient  $R^2$  (Table 2). Differences in  $R^2$  are especially small  
14 between  $N_{H\&S}$  and  $N_{FBAP}$ , because both make use of emission rates as a function of almost the  
15 same parameters ( $N_{FBAP}$  includes an additional  $T$ -dependence). Parameters  $b_1$  and  $b_2$  in eq. (8)  
16 are estimated to give fungal spore concentrations matching best with measured FBAP  
17 concentrations. At  $T = 275.82$  K,  $F_{H\&S}$  is equal to  $F_{FBAP}$ , and temperatures above this  
18 threshold (as it is the case for almost all locations) shift  $F_{FBAP}$  to give a larger emission flux.  
19 At meteorological conditions present for the selected cases, the second part of eq. (8)  
20 dominates over the first part by a factor of  $\sim 4$  and therefore temperature changes have only a  
21 secondary influence on the emission flux. Hence,  $R^2$  is similar for both emission  
22 parameterizations.

23 Possible causes for the bias of  $F_{H\&S}$  and  $F_{S\&D}$  may come from different assumptions made to  
24 determine the fungal spore concentrations in ambient air. The mass size distribution of  
25 mannitol, which is used as a chemical tracer for fungal spores by Heald and Spracklen (2009),  
26 peaks in their study at particle diameters of  $\sim 5$   $\mu\text{m}$ . Additionally to fungal spores, bacteria,  
27 algae, lichens, and plant fragments, can produce mannitol and some of these can contribute to  
28 PBAP concentrations at  $\sim 5$   $\mu\text{m}$ . Similar assumptions are made for this study by linking FBAP  
29 to fungal spores, but chemical tracers vary between both studies. Furthermore, both literature-  
30 based emission fluxes compare local measurements to concentrations simulated on a global  
31 scale. Additional biases may arise when using these fluxes on a regional scale.

1  
2  
3  
4  
5  
6  
7  
8  
9  
10  
11  
12  
13  
14  
15  
16  
17  
18  
19  
20  
21  
22  
23  
24  
25  
26  
27

### **3.3.3.4. Contribution of Fungal Spore to Near-surface Aerosol Composition**

For a comparison of simulated fungal spores to the dry aerosol chemical composition, the fungal spore mass concentration is calculated from the number concentration assuming monodisperse and spherical particles ( $\rho_p = 1 \text{ g/cm}^3$ ; section 2.1). The horizontally distributed near-surface (approximately 10 m above ground) fungal spore number concentration using  $F_{FBAP}$  is shown in Figure 10. Concentrations simulated at the measurement locations are considerably lower than the high surface concentrations in the southern part of the model domain.

The simulated mass concentrations of each chemical aerosol compound are averaged over the land areas of the model domain and the time period of late August 2010 (Figure 11). The total aerosol mass concentration is approximately  $2.5 \mu\text{g/m}^3$ . Fungal spores distribute in the domain with an average number concentration of  $26 \text{ L}^{-1}$  over land. This corresponds to an average mass concentration of fungal spores of  $0.37 \mu\text{g/m}^3$  which accounts for 15.4% of the total simulated aerosol mass. The total aerosol mass excludes mineral dust as one of the main contributors to the chemical aerosol composition, which might lower the fraction of fungal spore mass considerably. A list of mass concentrations of the simulated chemical aerosol compounds, including fungal spores occurring at the measurement site, is given in Table 3. The fraction of fungal spores simulated for these sites varies between 9% and 20%. FBAP mass concentrations calculated from the measured FBAP number concentrations are also listed in Table 3. Here, the same spherical particle diameter and particle density as for the fungal spore simulation is assumed. The FBAP number concentrations are averaged over the same time period as covered by the aerosol simulation. Their share of the aerosol mass ranges from 5% at Manchester up to 64% at Hyytiälä. For Karlsruhe and Killarney, the fractions calculated from the measurements are in good agreement with the fractions resulting from the simulated fungal spore mass concentrations.

#### 1 **4. Discussion and Conclusions**

2 FBAP measurements from four locations in Northern Europe were compared with simulated  
3 fungal spore concentrations. Fluorescent particles in the diameter range of 2 - 4  $\mu\text{m}$  are  
4 highest in number concentration of FBAP measurements at the rural site near Karlsruhe,  
5 Germany (Huffman et al., 2010; Pöschl et al., 2010; Huffman et al., 2012; Healy et al., 2012a;  
6 Toprak and Schnaiter, 2013; Huffman et al., 2013). The diameter range for peak FBAP  
7 concentration matches closely with the modal size of many species of fungal spores known to  
8 be present in airborne concentrations. Simulated fungal spores have been adjusted to match  
9 this diameter. Contrary to that, an increase in number concentration towards small particles  
10 has been reported for some FBAP measurement series, but only a small fraction of particles  
11 could be counted as bacteria cells (Gabey et al., 2011; Huffman et al., 2010).

12 Comparison of simulations and measurements at four locations and the correlation of FBAP  
13 concentrations to meteorological and surface conditions are expected to be most robust when  
14 applying identical methods and conditions at all locations. These conditions were not fulfilled  
15 in our study. On one hand, site characteristics vary between the stations, which may influence  
16 the sensitivity of PBAP emission to surrounding conditions. On the other hand, the  
17 measurements are made with different instruments. The measurement series at Karlsruhe,  
18 Germany, are done with a WIBS-4 instrument which includes technical improvements  
19 compared to the WIBS-3 used at Manchester, UK and Cork, Ireland (Gabey et al., 2010;  
20 Healy et al., 2012b). At Hyytiälä, Finland, and Killarney, Ireland, the UV-APS is used to  
21 determine the FBAP concentration. This variation may lead to different estimation of the  
22 FBAP concentration and within this case study WIBS may report FBAP at lower  
23 concentrations than UV-APS at different locations but similar meteorological conditions.

24 In this paper, fungal spore concentrations are calculated with the COSMO-ART atmospheric  
25 model by using literature-based emission parameterizations which adapt simulated global  
26 atmospheric concentration to mannitol measurements or spore colony counts (Heald and  
27 Spracklen, 2009; Sesartic and Dallafior, 2011). Although mannitol concentration can include  
28 contributions from other PBAP (e.g. insects, bacteria, and algae) and from lower plants, the  
29 association to fungal spore concentration is reasonable (Di Filippo et al., 2013). Some  
30 differences in the comparison may occur from the usage of FBAP concentrations as a  
31 representative for fungal spores. Overall, ~~T~~he temporal development of the literature-based

1 simulated fungus spore concentrations calculated by COSMO-ART approximately reproduces  
2 the measured FBAP concentrations.

3 By using a time-independent (but spatially varying) emission flux  $F_{S\&D}$ , every development in  
4 the local temporal pattern arises from meteorological influences. A similar cycle develops  
5 between constant ( $F_{S\&D}$ ) and time-independent ( $F_{H\&S}$  and  $F_{FBAP}$ ) simulated fungus spore  
6 concentrations, but the order of magnitude differs to varying extend. Therefore and from by  
7 visually comparing to simulated boundary layer height, aA diurnal cycle in the simulated  
8 fungus spore concentrations with a maximum between midnight and sunrise is probably  
9 influenced at least partly by boundary layer compression at night. Measured FBAP  
10 concentrations are often not consistent to simulated  $h_{PBL}$  which suggest that  $N_{F,c}$  is  
11 additionally influenced by increases in biological emission at night.

12 The purpose of the work reported here was to develop a new emission parameterization for  
13 fungus spores, because literature-based emissions for fungus spores have been found to  
14 significantly underestimate measured FBAP concentrations. The parameterization is therefore  
15 adjusted to the FBAP concentrations (section 3.2). As was formulated by Heald and  
16 Spracklen (2009), it depends on the specific humidity and the leaf area index, but is extended  
17 by temperature. The resulting concentrations are in better agreement to the measured FBAP  
18 concentrations on the average, but variations in the measurements are not always captured by  
19 the simulation. Another long-term analysis of FBAP concentrations and surrounding  
20 conditions may result in a further adjustment of the parameters or reveal another parameter  
21 driving the emission.

22 Using the new emission parameterization on a model domain for Europe, fungus spore  
23 emission fluxes are extrapolated from northern parts of the domain, where UV-LIF  
24 measurements were located, also to Southern Europe. There, much higher emission fluxes  
25 occur in the simulation, partially caused by higher specific humidity, which is also the case  
26 for  $F_{H\&S}$ , as well by temperature dependence in  $F_{FBAP}$ . This extrapolation is without local  
27 Southern European measurements, however, and thus further UV-LIF measurements are  
28 recommended for this region in Southern Europe where fungus spore emission fluxes are  
29 potentially greater.

30 As a result of the relatively low horizontal resolution, small-scale variations influencing  
31 fungus spore emission at the measurement sites may not be resolved. Influences on a small  
32 scale might be due to an increased amount of fungi for the given vegetation type. When

1 taking the leaf area index as a surrogate for the vegetation type, uncertainties may result from  
2 an insufficient relation to the presence of fungi or additional surrounding factors favoring  
3 fungi growth. Furthermore, variations in precipitation may not be captured by the model,  
4 which then may lead to improper fungal spore concentrations. The same holds for small wind  
5 gusts and convective cells which may have a strong influence on spore dispersion, but are not  
6 captured well in the model. An increase in fungal spore concentration during or shortly after  
7 rain events (Huffman et al., 2013) could not be reproduced by the simulations, as this effect is  
8 not included in the emission parameterization to an adequate extent.

9 The module calculating the dispersion of fungal spores does not include all processes of  
10 aerosol dynamics and cloud physics. Of the processes not included, only breaking up of  
11 spores can enhance their number concentration. Coagulation is neglected, as in most cases the  
12 fungal spore number concentration is low and, hence, their collision is highly improbable. A  
13 coagulation of spores with other aerosol particles is more likely to happen, but not included in  
14 the simulations. Not much is known about the role of fungal spores in clouds and their ability  
15 to act as cloud condensation nuclei.

16 The simulations presented in this paper highlight the importance of PBAP to the composition  
17 of atmospheric aerosol. Fungal spores, the focus of this paper, are among the main  
18 contributors to PBAP and therefore exert significant influence on aerosol loading. In this  
19 study, COSMO-ART is used up to simulate all major chemical aerosol compounds except for  
20 mineral dust in a domain covering Western Europe. When averaging the mass concentration  
21 horizontally across the land-covered part of the model domain and over all time steps of the  
22 simulation, fungal spores are among the major mass components (Figure 11). However, the  
23 fraction of fungal spores might be overestimated here, as another major aerosol component,  
24 mineral dust, is not included, because the domain does not include any desert dust source  
25 areas. At the selected cases, back trajectories with the HYSPLIT (Draxler and Rolph, 2013)  
26 suggest that transport of Sahara dust into the domain is low. An additional difference in the  
27 treatment of aerosol dynamics implies that spores in the simulation are assumed to be  
28 monodisperse with a diameter of 3  $\mu\text{m}$  without being subjected to sedimentation.

29 A FBAP mass concentration, estimated from measured FBAP number concentrations  
30 ( $d_p = 3 \mu\text{m}$ ;  $\rho_p = 1 \text{ g/cm}^3$ ), may reach up to 64% of simulated near-surface chemical aerosol  
31 mass components in rural areas of Finland (Table 3). In comparison to relations of PBAP to  
32 total aerosol concentrations given in literature, their volume fraction of particles larger than

1 0.2  $\mu\text{m}$  during one year of measurements at a remote site in Siberia reaches 28% on the  
2 average and at Mainz, Germany the volume fraction amounts to 22% (Matthias-Maser et al.,  
3 2000). Both of these fractions agree well with simulated mass fractions of this study for  
4 comparable locations, but simulated concentrations given in this study are much lower than  
5 total number concentrations given in Matthias-Maser et al. (2000). In contrast, the number  
6 and mass fractions in the Amazonian basin are above 80% and therefore much higher than in  
7 the highlighted urban and remote areas (Pöschl et al., 2010), but here the absolute  
8 concentrations are less and therefore in the order of magnitude given by the simulation of this  
9 study.

10 PBAP and especially fungal spores might account for a major part of the aerosol loading.  
11 Locally, a correlation between increasing FBAP and ice nuclei number concentration (Tobo et  
12 al., 2013) shows that future model studies of PBAP impacts on clouds are needed to  
13 determine their relevance to atmospheric ice nucleation.

14

## 15 **Acknowledgements**

16 We wish to thank Alexa Schnur for preliminary studies in connection with this paper and Max  
17 Bangert for technical support. We would like to thank the EMPA members, particularly  
18 Christoph Knote and Dominik Brunner, for providing the emission data of the chemical  
19 compounds. We also wish to acknowledge P. Aalto, V. Hiltunen, T. Petäjä, C. Schumacher,  
20 and M. Kulmala for assistance gathering and analyzing data. We acknowledge support by the  
21 Deutsche Forschungsgemeinschaft and the Open Access Publishing Fund of the Karlsruhe  
22 Institute of Technology. This research was funded by the Helmholtz Association through the  
23 Helmholtz Climate Initiative REKLIM, the President's Initiative and Networking Fund and  
24 by DFG through project HO 4612/1-1 (FOR 1525 INUIT). J. A. Huffman acknowledges  
25 internal faculty funding from the University of Denver. J. A. Huffman, C. Pöhlker, and U.  
26 Pöschl acknowledge financial support from the Max Planck Society (MPG), the Max Planck  
27 Graduate Center with the Johannes Gutenberg University Mainz (MPGC), the LEC Geocycles  
28 Mainz, and the German Research Foundation (DFG PO1013/5-1, FOR 1525 INUIT).

29

## 1 **References**

- 2 Ariya, P. A., Sun, J., Eltouny, N. A., Hudson, E. D., Hayes, C. T., and Kos, G.: Physical and chemical  
3 characterization of bioaerosols – Implications for nucleation processes, *International Reviews in*  
4 *Physical Chemistry*, 28, 1-32, 2009.
- 5 Aylor, D. E.: Settling speed of corn (*Zea mays*) pollen, *Journal of Aerosol Science*, 33, 1601-1607,  
6 [http://dx.doi.org/10.1016/S0021-8502\(02\)00105-2](http://dx.doi.org/10.1016/S0021-8502(02)00105-2), 2002.
- 7 Bartholomé, E., and Belward, A. S.: GLC2000: a new approach to global land cover mapping from  
8 Earth observation data, *International Journal of Remote Sensing*, 26, 1959-1977,  
9 [10.1080/01431160412331291297](https://doi.org/10.1080/01431160412331291297), 2005.
- 10 Bauer, H., Schueller, E., Weinke, G., Berger, A., Hitzemberger, R., Marr, I. L., and Puxbaum, H.:  
11 Significant contributions of fungal spores to the organic carbon and to the aerosol mass balance of  
12 the urban atmospheric aerosol, *Atmospheric Environment*, 42, 5542-5549,  
13 <http://dx.doi.org/10.1016/j.atmosenv.2008.03.019>, 2008.
- 14 Bones, D. L., Henricksen, D. K., Mang, S. A., Gonsior, M., Bateman, A. P., Nguyen, T. B., Cooper, W. J.,  
15 and Nizkorodov, S. A.: Appearance of strong absorbers and fluorophores in limonene-O<sub>3</sub> secondary  
16 organic aerosol due to NH<sub>4</sub><sup>+</sup>-mediated chemical aging over long time scales, *Journal of Geophysical*  
17 *Research: Atmospheres*, 115, D05203, [10.1029/2009jd012864](https://doi.org/10.1029/2009jd012864), 2010.
- 18 Brosseau, L. M., Vesley, D., Rice, N., Goodell, K., Nellis, M., and Hairston, P.: Differences in Detected  
19 Fluorescence Among Several Bacterial Species Measured with a Direct-Reading Particle Sizer and  
20 Fluorescence Detector, *Aerosol Science and Technology*, 32, 545-558, [10.1080/027868200303461](https://doi.org/10.1080/027868200303461),  
21 2000.
- 22 Burch, M., and Levetin, E.: Effects of meteorological conditions on spore plumes, *International*  
23 *Journal of Biometeorology*, 46, 107-117, [10.1007/s00484-002-0127-1](https://doi.org/10.1007/s00484-002-0127-1), 2002.
- 24 Burrows, S. M., Elbert, W., Lawrence, M. G., and Pöschl, U.: Bacteria in the global atmosphere – Part  
25 1: Review and synthesis of literature data for different ecosystems, *Atmos. Chem. Phys.*, 9, 9263-  
26 9280, [10.5194/acp-9-9263-2009](https://doi.org/10.5194/acp-9-9263-2009), 2009.
- 27 Caruana, D. J.: Detection and analysis of airborne particles of biological origin: present and future,  
28 *Analyst*, 136, 4641-4652, [10.1039/c1an15506g](https://doi.org/10.1039/c1an15506g), 2011.
- 29 Christner, B. C., Morris, C. E., Foreman, C. M., Cai, R., and Sands, D. C.: Ubiquity of Biological Ice  
30 Nucleators in Snowfall, *Science*, 319, 1214, [10.1126/science.1149757](https://doi.org/10.1126/science.1149757), 2008.
- 31 Creamean, J. M., Suski, K. J., Rosenfeld, D., Cazorla, A., DeMott, P. J., Sullivan, R. C., White, A. B.,  
32 Ralph, F. M., Minnis, P., Comstock, J. M., Tomlinson, J. M., and Prather, K. A.: Dust and Biological  
33 Aerosols from the Sahara and Asia Influence Precipitation in the Western U.S, *Science*, 339, 1572-  
34 1578, [10.1126/science.1227279](https://doi.org/10.1126/science.1227279), 2013.
- 35 DeLeon-Rodriguez, N., Latham, T. L., Rodriguez-R, L. M., Barazesh, J. M., Anderson, B. E., Beyersdorf,  
36 A. J., Ziemba, L. D., Bergin, M., Nenes, A., and Konstantinidis, K. T.: Microbiome of the upper  
37 troposphere: Species composition and prevalence, effects of tropical storms, and atmospheric  
38 implications, *Proceedings of the National Academy of Sciences*, 110, 2575-2580,  
39 [10.1073/pnas.1212089110](https://doi.org/10.1073/pnas.1212089110), 2013.
- 40 DeMott, P. J., and Prenni, A. J.: New Directions: Need for defining the numbers and sources of  
41 biological aerosols acting as ice nuclei, *Atmospheric Environment*, 44, 1944-1945, 2010.
- 42 Després, V. R., Huffman, J. A., Burrows, S. M., Hoose, C., Safatov, A. S., Buryak, G., Fröhlich-Nowoisky,  
43 J., Elbert, W., Andreae, M. O., Pöschl, U., and Jaenicke, R.: Primary biological aerosol particles in the  
44 atmosphere: a review, *Tellus B*, 64, 15598, [10.3402/tellusb.v64i0.15598](https://doi.org/10.3402/tellusb.v64i0.15598), 2012.

- 1 Di Filippo, P., Pomata, D., Riccardi, C., Buiarelli, F., and Perrino, C.: Fungal contribution to size-  
2 segregated aerosol measured through biomarkers, *Atmospheric Environment*, 64, 132-140,  
3 10.1016/j.atmosenv.2012.10.010, 2013.
- 4 Doms, G., and Schättler, U.: A Description of the Nonhydrostatic Regional COSMO-Model, Deutscher  
5 Wetterdienst, Offenbach, Germany, 2002.
- 6 Elbert, W., Taylor, P. E., Andreae, M. O., and Pöschl, U.: Contribution of fungi to primary biogenic  
7 aerosols in the atmosphere: wet and dry discharged spores, carbohydrates, and inorganic ions,  
8 *Atmos. Chem. Phys.*, 7, 4569-4588, 10.5194/acp-7-4569-2007, 2007.
- 9 Fang, Z. G., Ouyang, Z. Y., Zheng, H., and Wang, X. K.: Concentration and size distribution of  
10 culturable airborne microorganisms in outdoor environments in Beijing, China, *Aerosol Science and  
11 Technology*, 42, 325-334, 10.1080/02786820802068657, 2008.
- 12 Foot, V. E., Kaye, P. H., Stanley, W. R., Barrington, S. J., Gallagher, M., and Gabey, A.: Low-cost real-  
13 time multiparameter bio-aerosol sensors, *Optically Based Biological and Chemical Detection for  
14 Defence IV*, 7116, 71160I-71112, 2008.
- 15 Forster, P., Ramaswamy, V., Artaxo, P., Berntsen, T., Betts, R., Fahey, D. W., Haywood, J., Lean, J.,  
16 Lowe, D. C., Myhre, G., Nganga, J., Prinn, R., Raga, G., Schulz, M., and Dorland, R. V.: Changes in  
17 Atmospheric Constituents and in Radiative Forcing, in: *Climate Change 2007: The Physical Science  
18 Basis. Contribution of Working Group I to the Fourth Assessment Report of the Intergovernmental  
19 Panel on Climate Change*, edited by: Solomon, S., Qin, D., Manning, M., Chen, Z., Marquis, M., Averyt,  
20 K. B., M.Tignor, and (eds.), H. L. M., Cambridge University Press, Cambridge, United Kingdom and  
21 New York, NY, USA, 2007.
- 22 Fountoukis, C., and Nenes, A.: ISORROPIA II: a computationally efficient thermodynamic equilibrium  
23 model for  $K^+$  -  $Ca^{2+}$  -  $Mg^{2+}$  -  $NH_4^+$  -  $Na^+$  -  $SO_4^{2-}$  -  $NO_3^-$  -  $Cl^-$  -  $H_2O$  aerosols, *Atmos. Chem. Phys.*, 7, 4639-  
24 4659, 10.5194/acp-7-4639-2007, 2007.
- 25 Fröhlich-Nowoisky, J., Burrows, S. M., Xie, Z., Engling, G., Solomon, P. A., Fraser, M. P., Mayol-  
26 Bracero, O. L., Artaxo, P., Begerow, D., Conrad, R., Andreae, M. O., Després, V. R., and Pöschl, U.:  
27 Biogeography in the air: fungal diversity over land and oceans, *Biogeosciences*, 9, 1125-1136,  
28 10.5194/bg-9-1125-2012, 2012.
- 29 Gabey, A. M., Gallagher, M. W., Whitehead, J., Dorsey, J. R., Kaye, P. H., and Stanley, W. R.:  
30 Measurements and comparison of primary biological aerosol above and below a tropical forest  
31 canopy using a dual channel fluorescence spectrometer, *Atmospheric Chemistry and Physics*, 10,  
32 4453-4466, 10.5194/acp-10-4453-2010, 2010.
- 33 Gabey, A. M., Stanley, W. R., Gallagher, M. W., and Kaye, P. H.: The fluorescence properties of  
34 aerosol larger than 0.8  $\mu m$  in urban and tropical rainforest locations, *Atmos. Chem. Phys.*, 11, 5491-  
35 5504, 10.5194/acp-11-5491-2011, 2011.
- 36 Gabey, A. M., Vaitilingom, M., Freney, E., Boulon, J., Sellegri, K., Gallagher, M. W., Crawford, I. P.,  
37 Robinson, N. H., Stanley, W. R., and Kaye, P. H.: Observations of fluorescent and biological aerosol at  
38 a high-altitude site in central France, *Atmos. Chem. Phys.*, 13, 7415-7428, 10.5194/acp-13-7415-  
39 2013, 2013.
- 40 Graham, B., Guyon, P., Maenhaut, W., Taylor, P. E., Ebert, M., Matthias-Maser, S., Mayol-Bracero, O.  
41 L., Godoi, R. H. M., Artaxo, P., Meixner, F. X., Moura, M. A. L., Rocha, C. H. E. D. A., Grieken, R. V.,  
42 Glovsky, M. M., Flagan, R. C., and Andreae, M. O.: Composition and diurnal variability of the natural  
43 Amazonian aerosol, *Journal of Geophysical Research: Atmospheres*, 108, 4765,  
44 10.1029/2003jd004049, 2003.

- 1 Gregory, P. H.: The microbiology of the atmosphere, Plant Science Monographs, edited by: Polunin,  
2 N., Leonard Hill, London, 1961.
- 3 Haga, D. I., Iannone, R., Wheeler, M. J., Mason, R., Polishchuk, E. A., Fetch, T., van der Kamp, B. J.,  
4 McKendry, I. G., and Bertram, A. K.: Ice nucleation properties of rust and bunt fungal spores and their  
5 transport to high altitudes where they can cause heterogeneous freezing, *Journal of Geophysical*  
6 *Research: Atmospheres*, n/a-n/a, 10.1002/jgrd.50556, 2013.
- 7 Hairston, P. P., Ho, J., and Quant, F. R.: Design of an instrument for real-time detection of bioaerosols  
8 using simultaneous measurement of particle aerodynamic size and intrinsic fluorescence, *J Aerosol*  
9 *Sci*, 28, 471-482, 1997.
- 10 Hameed, A. A. A., and Khodr, M. I.: Suspended particulates and bioaerosols emitted from an  
11 agricultural non-point source, *J. Environ. Monit.*, 3, 206-209, 2001.
- 12 Heald, C. L., and Spracklen, D. V.: Atmospheric budget of primary biological aerosol particles from  
13 fungal spores, *Geophys. Res. Lett.*, 36, L09806, 10.1029/2009gl037493, 2009.
- 14 Healy, D. A., O'Connor, D. J., Burke, A. M., and Sodeau, J. R.: A laboratory assessment of the  
15 Waveband Integrated Bioaerosol Sensor (WIBS-4) using individual samples of pollen and fungal spore  
16 material, *Atmospheric Environment*, 60, 534-543,  
17 <http://dx.doi.org/10.1016/j.atmosenv.2012.06.052>, 2012a.
- 18 Healy, D. A., O'Connor, D. J., and Sodeau, J. R.: Measurement of the particle counting efficiency of  
19 the "Waveband Integrated Bioaerosol Sensor" model number 4 (WIBS-4), *Journal of Aerosol Science*,  
20 47, 94-99, <http://dx.doi.org/10.1016/j.jaerosci.2012.01.003>, 2012b.
- 21 Healy, D. A., Huffman, J. A., O'Connor, D. J., Pöhlker, C., Pöschl, U., and Sodeau, J. R.: Ambient  
22 measurements of biological aerosol particles near Killarney, Ireland: a comparison between real-time  
23 fluorescence and microscopy techniques, *Atmos. Chem. Phys. Discuss.*, 14, 3875-3915,  
24 10.5194/acpd-14-3875-2014, 2014.
- 25 Helbig, N., Vogel, B., Vogel, H., and Fiedler, F.: Numerical modelling of pollen dispersion on the  
26 regional scale, *Aerobiologia*, 20, 3-19, 10.1023/b:aero.0000022984.51588.30, 2004.
- 27 Hoose, C., Kristjánsson, J. E., and Burrows, S. M.: How important is biological ice nucleation in clouds  
28 on a global scale?, *Environmental Research Letters*, 5, 024009, 2010a.
- 29 Hoose, C., Kristjánsson, J. E., Chen, J.-P., and Hazra, A.: A Classical-Theory-Based Parameterization of  
30 Heterogeneous Ice Nucleation by Mineral Dust, Soot, and Biological Particles in a Global Climate  
31 Model, *Journal of the Atmospheric Sciences*, 67, 2483-2503, 10.1175/2010jas3425.1, 2010b.
- 32 Hoose, C., and Möhler, O.: Heterogeneous ice nucleation on atmospheric aerosols: a review of  
33 results from laboratory experiments, *Atmos. Chem. Phys.*, 12, 9817-9854, 10.5194/acp-12-9817-  
34 2012, 2012.
- 35 Huffman, J. A., Treutlein, B., and Pöschl, U.: Fluorescent biological aerosol particle concentrations  
36 and size distributions measured with an Ultraviolet Aerodynamic Particle Sizer (UV-APS) in Central  
37 Europe, *Atmospheric Chemistry and Physics*, 10, 3215-3233, 2010.
- 38 Huffman, J. A., Sinha, B., Garland, R. M., Snee-Pollmann, A., Gunthe, S. S., Artaxo, P., Martin, S. T.,  
39 Andreae, M. O., and Pöschl, U.: Size distributions and temporal variations of biological aerosol  
40 particles in the Amazon rainforest characterized by microscopy and real-time UV-APS fluorescence  
41 techniques during AMAZE-08, *Atmos. Chem. Phys.*, 12, 11997-12019, 10.5194/acp-12-11997-2012,  
42 2012.
- 43 Huffman, J. A., Prenni, A. J., DeMott, P. J., Pöhlker, C., Mason, R. H., Robinson, N. H., Fröhlich-  
44 Nowoisky, J., Tobo, Y., Després, V. R., Garcia, E., Gochis, D. J., Harris, E., Müller-Germann, I., Ruzene,

1 C., Schmer, B., Sinha, B., Day, D. A., Andreae, M. O., Jimenez, J. L., Gallagher, M., Kreidenweis, S. M.,  
2 Bertram, A. K., and Pöschl, U.: High concentrations of biological aerosol particles and ice nuclei  
3 during and after rain, *Atmos. Chem. Phys.*, 13, 6151-6164, 10.5194/acp-13-6151-2013, 2013.

4 Im, U., Christodoulaki, S., Violaki, K., Zarnpas, P., Kocak, M., Daskalakis, N., Mihalopoulos, N., and  
5 Kanakidou, M.: Atmospheric deposition of nitrogen and sulfur over southern Europe with focus on  
6 the Mediterranean and the Black Sea, *Atmospheric Environment*, 81, 660-670,  
7 <http://dx.doi.org/10.1016/j.atmosenv.2013.09.048>, 2013.

8 Jacobson, M. Z., and Streets, D. G.: Influence of future anthropogenic emissions on climate, natural  
9 emissions, and air quality, *Journal of Geophysical Research: Atmospheres*, 114, D08118,  
10 10.1029/2008jd011476, 2009.

11 Jaenicke, R.: Über die Dynamik atmosphärischer Aitkenteilchen, in: *Berichte der Bunsengesellschaft  
12 für physikalische Chemie*, 11, Wiley-VCH Verlag GmbH & Co. KGaA, 1198-1202, 1978.

13 Jaenicke, R., Matthias-Maser, S., and Gruber, S.: Omnipresence of biological material in the  
14 atmosphere, *Environmental Chemistry*, 4, 217-220, <http://dx.doi.org/10.1071/EN07021>, 2007.

15 Jones, A. M., and Harrison, R. M.: The effects of meteorological factors on atmospheric bioaerosol  
16 concentrations--a review, *Science of The Total Environment*, 326, 151-180,  
17 10.1016/j.scitotenv.2003.11.021, 2004.

18 Kaye, P., Stanley, W. R., Hirst, E., Foot, E. V., Baxter, K. L., and Barrington, S. J.: Single particle  
19 multichannel bio-aerosol fluorescence sensor, *Opt. Express*, 13, 3583-3593,  
20 10.1364/opex.13.003583, 2005.

21 Knote, C., Brunner, D., Vogel, H., Allan, J., Asmi, A., Äijälä, M., Carbone, S., van der Gon, H. D.,  
22 Jimenez, J. L., Kiendler-Scharr, A., Mohr, C., Poulain, L., Prévôt, A. S. H., Swietlicki, E., and Vogel, B.:  
23 Towards an online-coupled chemistry-climate model: evaluation of trace gases and aerosols in  
24 COSMO-ART, *Geosci. Model Dev.*, 4, 1077-1102, 10.5194/gmd-4-1077-2011, 2011.

25 Kuenen, J., Denier van der Gon, H., Visschedijk, A., van der Brugh, H., and Gijlswijk, R.: MACC  
26 European emission inventory for the years 2003–2007, TNO, Utrecht, Netherlands, TNO-060-UT-  
27 2011-00588, 49, 2011.

28 Lee, H. J., Laskin, A., Laskin, J., and Nizkorodov, S. A.: Excitation–Emission Spectra and Fluorescence  
29 Quantum Yields for Fresh and Aged Biogenic Secondary Organic Aerosols, *Environmental Science &  
30 Technology*, 47, 5763-5770, 10.1021/es400644c, 2013.

31 Lin, W.-H., and Li, C.-S.: Size Characteristics of Fungus Allergens in the Subtropical Climate, *Aerosol  
32 Science and Technology*, 25, 93-100, 10.1080/02786829608965382, 1996.

33 Lundgren, K., Vogel, B., Vogel, H., and Kottmeier, C.: Direct radiative effects of sea salt for the  
34 Mediterranean region under conditions of low to moderate wind speeds, *Journal of Geophysical  
35 Research: Atmospheres*, 118, 1906-1923, 10.1029/2012jd018629, 2013.

36 Mahowald, N., Jickells, T. D., Baker, A. R., Artaxo, P., Benitez-Nelson, C. R., Bergametti, G., Bond, T. C.,  
37 Chen, Y., Cohen, D. D., Herut, B., Kubilay, N., Losno, R., Luo, C., Maenhaut, W., McGee, K. A., Okin, G.  
38 S., Siefert, R. L., and Tsukuda, S.: Global distribution of atmospheric phosphorus sources,  
39 concentrations and deposition rates, and anthropogenic impacts, *Global Biogeochemical Cycles*, 22,  
40 GB4026, 10.1029/2008gb003240, 2008.

41 Martin, S. T., Andreae, M. O., Artaxo, P., Baumgardner, D., Chen, Q., Goldstein, A. H., Guenther, A.,  
42 Heald, C. L., Mayol-Bracero, O. L., McMurry, P. H., Pauliquevis, T., Pöschl, U., Prather, K. A., Roberts,  
43 G. C., Saleska, S. R., Silva Dias, M. A., Spracklen, D. V., Swietlicki, E., and Trebs, I.: Sources and  
44 properties of Amazonian aerosol particles, *Reviews of Geophysics*, 48, RG2002,  
45 10.1029/2008rg000280, 2010.

1 Matthias-Maser, S., Obolkin, V., Khodzer, T., and Jaenicke, R.: Seasonal variation of primary biological  
2 aerosol particles in the remote continental region of Lake Baikal/Siberia, *Atmospheric Environment*,  
3 34, 3805-3811, 10.1016/s1352-2310(00)00139-4, 2000.

4 Morris, C. E., Georgakopoulos, D. G., and Sands, D. C.: Ice nucleation active bacteria and their  
5 potential role in precipitation, *J. Phys. IV France*, 121, 87-103, 2004.

6 Morris, C. E., Sands, D. C., Glaux, C., Samsatly, J., Asaad, S., Moukahel, A. R., Gonçalves, F. L. T., and  
7 Bigg, E. K.: Urediospores of rust fungi are ice nucleation active at  $> -10$  °C and harbor ice nucleation  
8 active bacteria, *Atmos. Chem. Phys.*, 13, 4223-4233, 10.5194/acp-13-4223-2013, 2013.

9 Murray, B. J., O'Sullivan, D., Atkinson, J. D., and Webb, M. E.: Ice nucleation by particles immersed in  
10 supercooled cloud droplets, *Chemical Society Reviews*, 41, 6519-6554, 2012.

11 Olson, D. M., Dinerstein, E., Wikramanayake, E. D., Burgess, N. D., Powell, G. V. N., Underwood, E. C.,  
12 D'Amico, J. A., Itoua, I., Strand, H. E., Morrison, J. C., Loucks, C. J., Allnutt, T. F., Ricketts, T. H., Kura,  
13 Y., Lamoreux, J. F., Wettengel, W. W., Hedao, P., and Kassem, K. R.: Terrestrial Ecoregions of the  
14 World: A New Map of Life on Earth, *BioScience*, 51, 933-938, 10.1641/0006-  
15 3568(2001)051[0933:teotwa]2.0.co;2, 2001.

16 Pan, Y.-I., Holler, S., Chang, R. K., Hill, S. C., Pinnick, R. G., Niles, S., and Bottiger, J. R.: Single-shot  
17 fluorescence spectra of individual micrometer-sized bioaerosols illuminated by a 351- or a 266-nm  
18 ultraviolet laser, *Opt. Lett.*, 24, 116-118, 10.1364/ol.24.000116, 1999.

19 Penner, J. E.: Carbonaceous aerosols influencing atmospheric radiation: black and organic carbon, in:  
20 *Aerosol Forcing of Climate*, edited by: Charlson, R. J. a. H., J., John Wiley and Sons, Chichester, 91 -  
21 108, 1995.

22 Petters, M. D., and Kreidenweis, S. M.: A single parameter representation of hygroscopic growth and  
23 cloud condensation nucleus activity, *Atmos. Chem. Phys.*, 7, 1961-1971, 10.5194/acp-7-1961-2007,  
24 2007.

25 Pöhlker, C., Huffman, J. A., and Pöschl, U.: Autofluorescence of atmospheric bioaerosols – fluorescent  
26 biomolecules and potential interferences, *Atmos. Meas. Tech.*, 5, 37-71, 10.5194/amt-5-37-2012,  
27 2012.

28 Pöhlker, C., Huffman, J. A., Förster, J. D., and Pöschl, U.: Autofluorescence of atmospheric  
29 bioaerosols: spectral fingerprints and taxonomic trends of pollen, *Atmos. Meas. Tech.*, 6, 3369-3392,  
30 10.5194/amt-6-3369-2013, 2013.

31 Pope, F. D.: Pollen grains are efficient cloud condensation nuclei, *Environmental Research Letters*, 5,  
32 044015, 2010.

33 Pöschl, U., Martin, S. T., Sinha, B., Chen, Q., Gunthe, S. S., Huffman, J. A., Borrmann, S., Farmer, D. K.,  
34 Garland, R. M., Helas, G., Jimenez, J. L., King, S. M., Manzi, A., Mikhailov, E., Pauliquevis, T., Petters,  
35 M. D., Prenni, A. J., Roldin, P., Rose, D., Schneider, J., Su, H., Zorn, S. R., Artaxo, P., and Andreae, M.  
36 O.: Rainforest Aerosols as Biogenic Nuclei of Clouds and Precipitation in the Amazon, *Science*, 329,  
37 1513-1516, 10.1126/science.1191056, 2010.

38 Prenni, A. J., Petters, M. D., Kreidenweis, S. M., Heald, C. L., Martin, S. T., Artaxo, P., Garland, R. M.,  
39 Wollny, A. G., and Poschl, U.: Relative roles of biogenic emissions and Saharan dust as ice nuclei in  
40 the Amazon basin, *Nature Geosci*, 2, 402-405, 2009.

41 Prenni, A. J., Tobo, Y., Garcia, E., DeMott, P. J., Huffman, J. A., McCluskey, C. S., Kreidenweis, S. M.,  
42 Prenni, J. E., Pöhlker, C., and Pöschl, U.: The impact of rain on ice nuclei populations at a forested site  
43 in Colorado, *Geophysical Research Letters*, 40, 227-231, 10.1029/2012gl053953, 2013.

- 1 Ramankutty, N., Evan, A. T., Monfreda, C., and Foley, J. A.: Farming the planet: 1. Geographic  
2 distribution of global agricultural lands in the year 2000, *Global Biogeochem. Cycles*, 22, GB1003,  
3 10.1029/2007gb002952, 2008.
- 4 Reponen, T., Grinshpun, S. A., Conwell, K. L., Wiest, J., and Anderson, M.: Aerodynamic versus  
5 physical size of spores: Measurement and implication for respiratory deposition, *Grana*, 40, 119-125,  
6 10.1080/00173130152625851, 2001.
- 7 Rinke, R.: Parametrisierung des Auswaschens von Aerosolpartikeln durch Niederschlag, Ph.D. thesis,  
8 Inst. für Meteorol. und Klimaforsch., Univ. Karlsruhe (TH), Karlsruhe, Germany, 2008.
- 9 Robinson, N. H., Allan, J. D., Huffman, J. A., Kaye, P. H., Foot, V. E., and Gallagher, M.: Cluster analysis  
10 of WIBS single-particle bioaerosol data, *Atmos. Meas. Tech.*, 6, 337-347, 10.5194/amt-6-337-2013,  
11 2013.
- 12 Saari, S. E., Putkiranta, M. J., and Keskinen, J.: Fluorescence spectroscopy of atmospherically relevant  
13 bacterial and fungal spores and potential interferences, *Atmospheric Environment*, 71, 202-209,  
14 <http://dx.doi.org/10.1016/j.atmosenv.2013.02.023>, 2013.
- 15 Schell, B., Ackermann, I. J., Hass, H., Binkowski, F. S., and Ebel, A.: Modeling the formation of  
16 secondary organic aerosol within a comprehensive air quality model system, *Journal of Geophysical  
17 Research: Atmospheres*, 106, 28275-28293, 10.1029/2001jd000384, 2001.
- 18 Schumacher, C. J., Pöhlker, C., Aalto, P., Hiltunen, V., Petäjä, T., Kulmala, M., Pöschl, U., and Huffman,  
19 J. A.: Seasonal cycles of fluorescent biological aerosol particles in boreal and semi-arid forests of  
20 Finland and Colorado, *Atmos. Chem. Phys.*, 13, 11987-12001, 10.5194/acp-13-11987-2013, 2013.
- 21 Seinfeld, J. H., and Pandis, S. N.: *Atmospheric Chemistry and Physics - From Air Pollution to Climate  
22 Change (2nd Edition)*, John Wiley & Sons, Hoboken, New Jersey, USA, 2006.
- 23 Sesartic, A., and Dallafior, T. N.: Global fungal spore emissions, review and synthesis of literature  
24 data, *Biogeosciences*, 8, 1181-1192, 10.5194/bg-8-1181-2011, 2011.
- 25 Sesartic, A., Lohmann, U., and Storelvmo, T.: Bacteria in the ECHAM5-HAM global climate model,  
26 *Atmos. Chem. Phys.*, 12, 8645-8661, 10.5194/acp-12-8645-2012, 2012.
- 27 Shaffer, B. T., and Lighthart, B.: Survey of Culturable Airborne Bacteria at Four Diverse Locations in  
28 Oregon: Urban, Rural, Forest, and Coastal, *Microbial Ecology*, 34, 167-177, 10.2307/4251522, 1997.
- 29 Spracklen, D. V., and Heald, C. L.: The contribution of fungal spores and bacteria to regional and  
30 global aerosol number and ice nucleation immersion freezing rates, *Atmos. Chem. Phys. Discuss.*, 13,  
31 32459-32481, 10.5194/acpd-13-32459-2013, 2013.
- 32 Tobo, Y., Prenni, A. J., DeMott, P. J., Huffman, J. A., McCluskey, C. S., Tian, G., Pöhlker, C., Pöschl, U.,  
33 and Kreidenweis, S. M.: Biological aerosol particles as a key determinant of ice nuclei populations in a  
34 forest ecosystem, *Journal of Geophysical Research: Atmospheres*, n/a-n/a, 10.1002/jgrd.50801,  
35 2013.
- 36 Toprak, E., and Schnaiter, M.: Fluorescent biological aerosol particles measured with the Waveband  
37 Integrated Bioaerosol Sensor WIBS-4: laboratory tests combined with a one year field study, *Atmos.  
38 Chem. Phys.*, 13, 225-243, 10.5194/acp-13-225-2013, 2013.
- 39 Trail, F., Gaffoor, I., and Vogel, S.: Ejection mechanics and trajectory of the ascospores of *Gibberella  
40 zae* (anamorph *Fuarium graminearum*), *Fungal Genetics and Biology*, 42, 528-533,  
41 10.1016/j.fgb.2005.03.008, 2005.
- 42 Vogel, B., Vogel, H., Bäumer, D., Bangert, M., Lundgren, K., Rinke, R., and Stanelle, T.: The  
43 comprehensive model system COSMO-ART – radiative impact of aerosol on the state of the

1 atmosphere on the regional scale, *Atmos. Chem. Phys.*, 9, 14483-14528, 10.5194/acpd-9-14483-  
2 2009, 2009.

3 Vogel, H., Pauling, A., and Vogel, B.: Numerical simulation of birch pollen dispersion with an  
4 operational weather forecast system, *International Journal of Biometeorology*, 52, 805-814,  
5 10.1007/s00484-008-0174-3, 2008.

6 Winiwarter, W., Bauer, H., Caseiro, A., and Puxbaum, H.: Quantifying emissions of primary biological  
7 aerosol particle mass in Europe, *Atmospheric Environment*, 43, 1403-1409,  
8 <http://dx.doi.org/10.1016/j.atmosenv.2008.01.037>, 2009.

9 Yamamoto, N., Bibby, K., Qian, J., Hospodsky, D., Rismani-Yazdi, H., Nazaroff, W. W., and Peccia, J.:  
10 Particle-size distributions and seasonal diversity of allergenic and pathogenic fungi in outdoor air,  
11 *ISME J*, 6, 1801-1811, 2012.

12

13

1 Table 1. Overview of the measurement sites, including their geographical location and the types of instrument  
2 used ( $d_p$  corresponds to the optical particle diameter and  $d_a$  to the aerodynamic particle diameter). The sections  
3 below show the simulation periods and the availability of data at this site (filled dot). Mean values for the  
4 simulated meteorological and surface conditions used for the new emission parameterization (section 3.2) at the  
5 measurement site during the corresponding time periods are added to each section.

location	Karlsruhe, Germany	Hyytiälä, Finland	Manchester, UK	Killarney, Ireland
coordinates	49° 5' 43.6" N 8° 25' 45.0" E	61° 50' 41.0" N 24° 17' 17.4" E	53° 27' 57.0" N 2° 13' 56.0" W	52° 3' 28.0" N 9° 30' 16.4" W
altitude	111 m a.s.l.	152 m a.s.l.	45 m a.s.l.	34 m a.s.l.
instrument	WIBS-4	UV-APS	WIBS-3	UV-APS
size range	$0.8 \leq d_p \leq 16 \mu\text{m}$	$1 < d_a \leq 20 \mu\text{m}$	$0.8 \leq d_p \leq 20 \mu\text{m}$	$1 < d_a \leq 20 \mu\text{m}$
22 July 2010 - 28 July 2010	●	●	○	○
LAI ( $\text{m}^2/\text{m}^2$ )	3.18	3.72	-	-
mean T ( $^{\circ}\text{C}$ )	17.3	16.2	-	-
mean $q_v$ (kg/kg)	0.0088	0.0108	-	-
26 August 2010 - 01 September 2010	●	●	●	●
LAI ( $\text{m}^2/\text{m}^2$ )	2.94	3.4	2.87	2.06
mean T ( $^{\circ}\text{C}$ )	16.6	8.5	11.6	11.1
mean $q_v$ (kg/kg)	0.0099	0.0067	0.0073	0.0072
11 October 2010 - 21 October 2010	●	●	○	○
LAI ( $\text{m}^2/\text{m}^2$ )	1.49	1.27	-	-
mean T ( $^{\circ}\text{C}$ )	6.5	-0.6	-	-
mean $q_v$ (kg/kg)	0.0055	0.0034	-	-

6

7

1 Table 2. Correlation coefficient ( $R^2$ ) and normalized mean bias (NMB) for correlations between fungal spore and  
 2 FBAP concentrations at different locations and three different time periods

	$N_{H\&S}$		$N_{S\&D}$		$N_{FBAP}$	
	$R^2$	$NMB$	$R^2$	$NMB$	$R^2$	$NMB$
Karlsruhe, Jul10	0.0047	-57.54	0.0127	-66.30	0.0048	-31.86
Karlsruhe, Aug10	0.0125	-63.82	0.0002	20.14	0.0274	-34.68
Karlsruhe, Oct10	0.0125	-35.71	0.0052	-40.08	0.0124	1.36
Hyytiälä, Jul10	0.3268	3.18	0.3358	-67.49	0.3255	50.50
Hyytiälä, Aug10	0.0002	-57.54	0.0099	35.43	0.0511	-59.04
Hyytiälä, Oct10	0.0016	-61.74	0.0350	-75.56	0.0000	-45.97
Manchester, Aug10	0.4558	2.74	0.4274	37.72	0.4409	63.26
Killarney, Aug10	0.2408	84.42	0.0998	200.51	0.1982	213.81
<b>all</b>	<b>0.1834</b>	<b>-44.04</b>	<b>0.0551</b>	<b>-28.74</b>	<b>0.1877</b>	<b>-0.43</b>

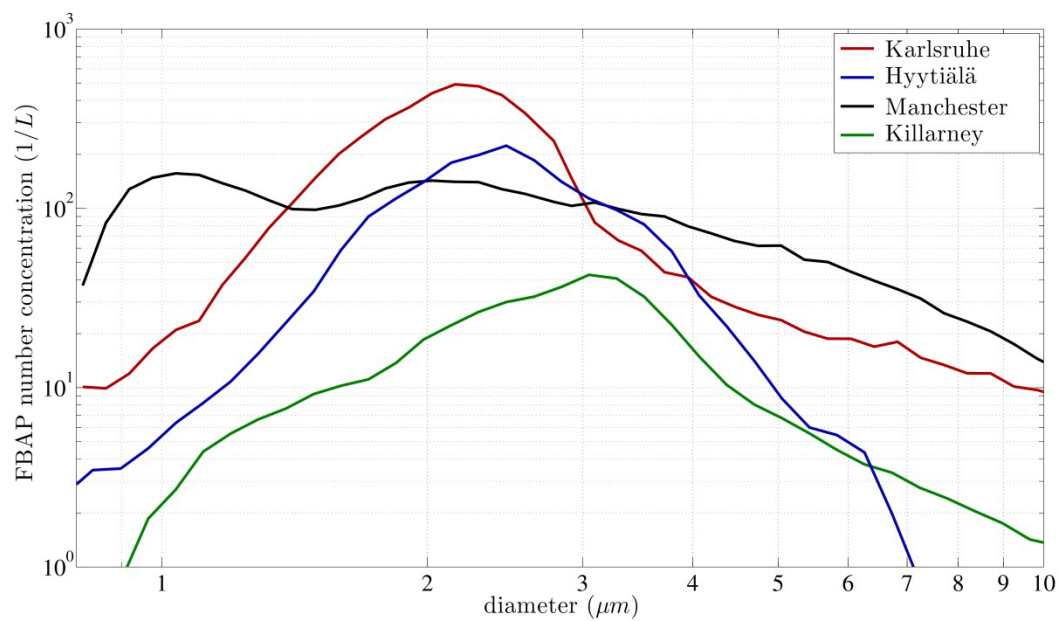
3

4

1 Table 3. Simulated aerosol mass concentrations for aerosol chemical components, including fungal spores,  
 2 together with measured FBAP values in  $\mu\text{g}/\text{m}^3$  at the measuring sites as averages over the time period during  
 3 August 2010

Particle Mass ( $\mu\text{g}/\text{m}^3$ )	Karlsruhe, Germany	Hyytiälä, Finland	Manchester, UK	Killarney, Ireland
measured FBAP	0.46	0.81	0.19	0.19
simulated fungal spores	0.41	0.20	0.35	0.28
sea salt	0.44	0.01	1.62	1.11
soot	0.19	0.06	0.42	0.04
$\text{SO}_4^{2-}$	0.18	0.01	0.11	0.05
$\text{NH}_4^+$	0.44	0.01	0.14	0.07
$\text{NO}_3^-$	1.29	0.01	0.34	0.18
SOA	0.41	0.24	0.14	0.04
aPOA	0.67	0.13	0.85	0.11

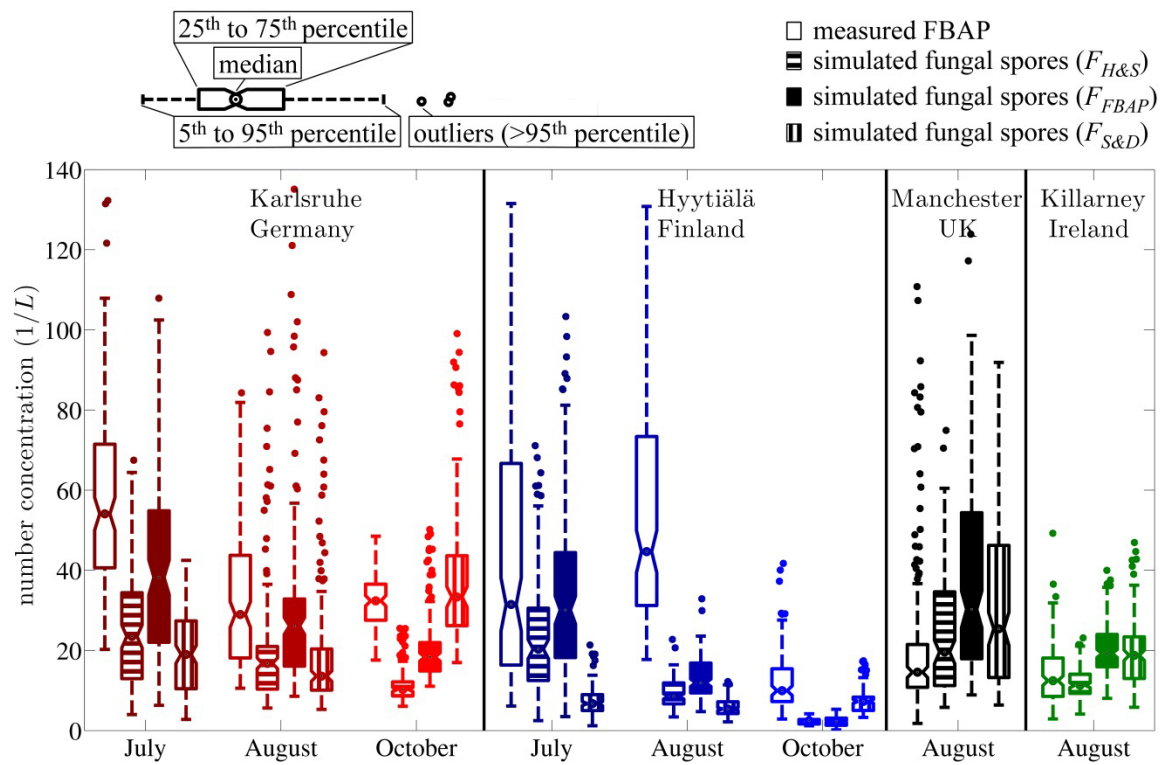
4  
5



1

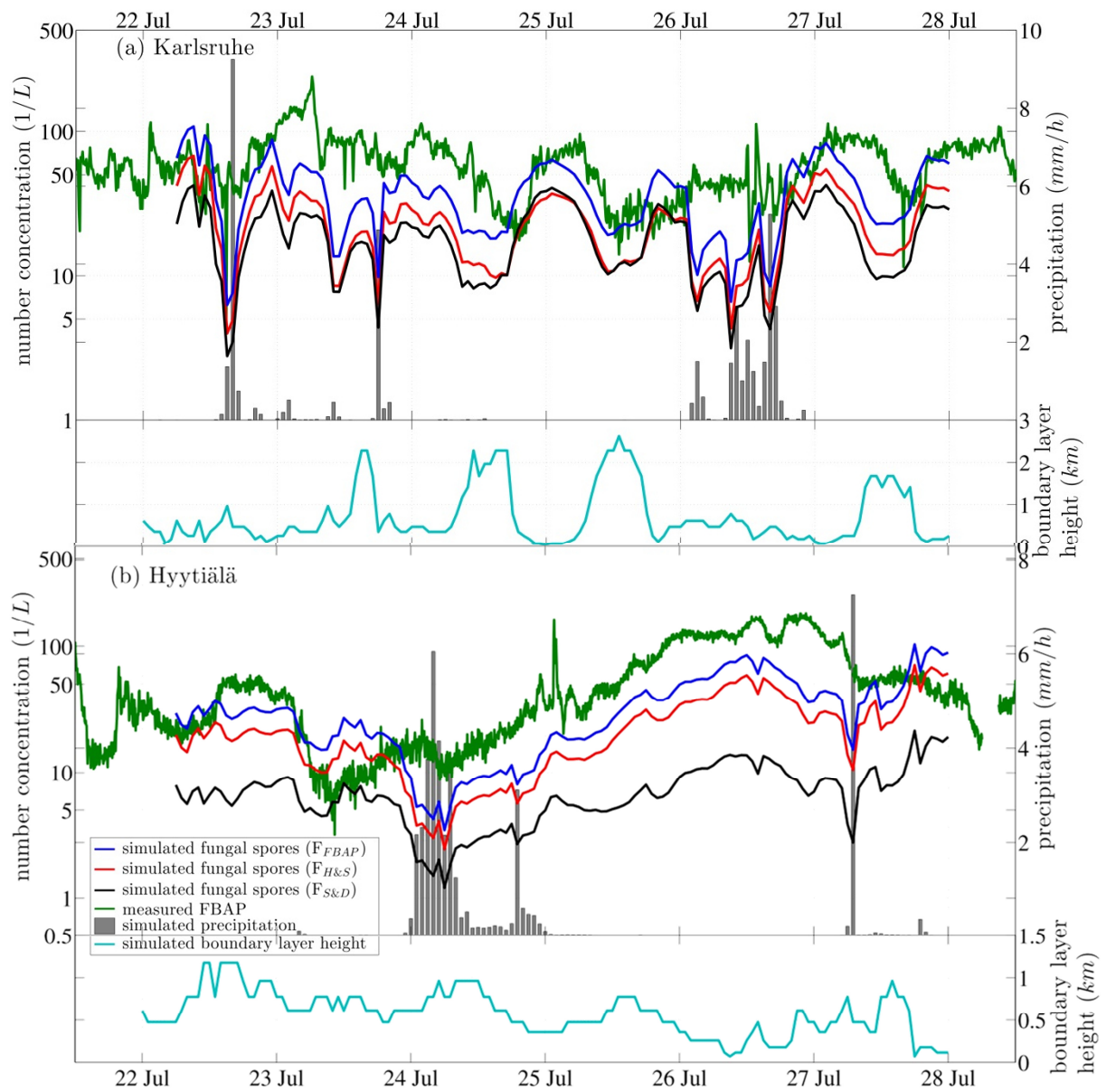
2 Figure 1. Average FBAP size distributions derived from UV-LIF measurements during case studies in August  
 3 2010 at Karlsruhe (Germany), Hyytiälä (Finland), Manchester (UK), and Killarney (Ireland).

4



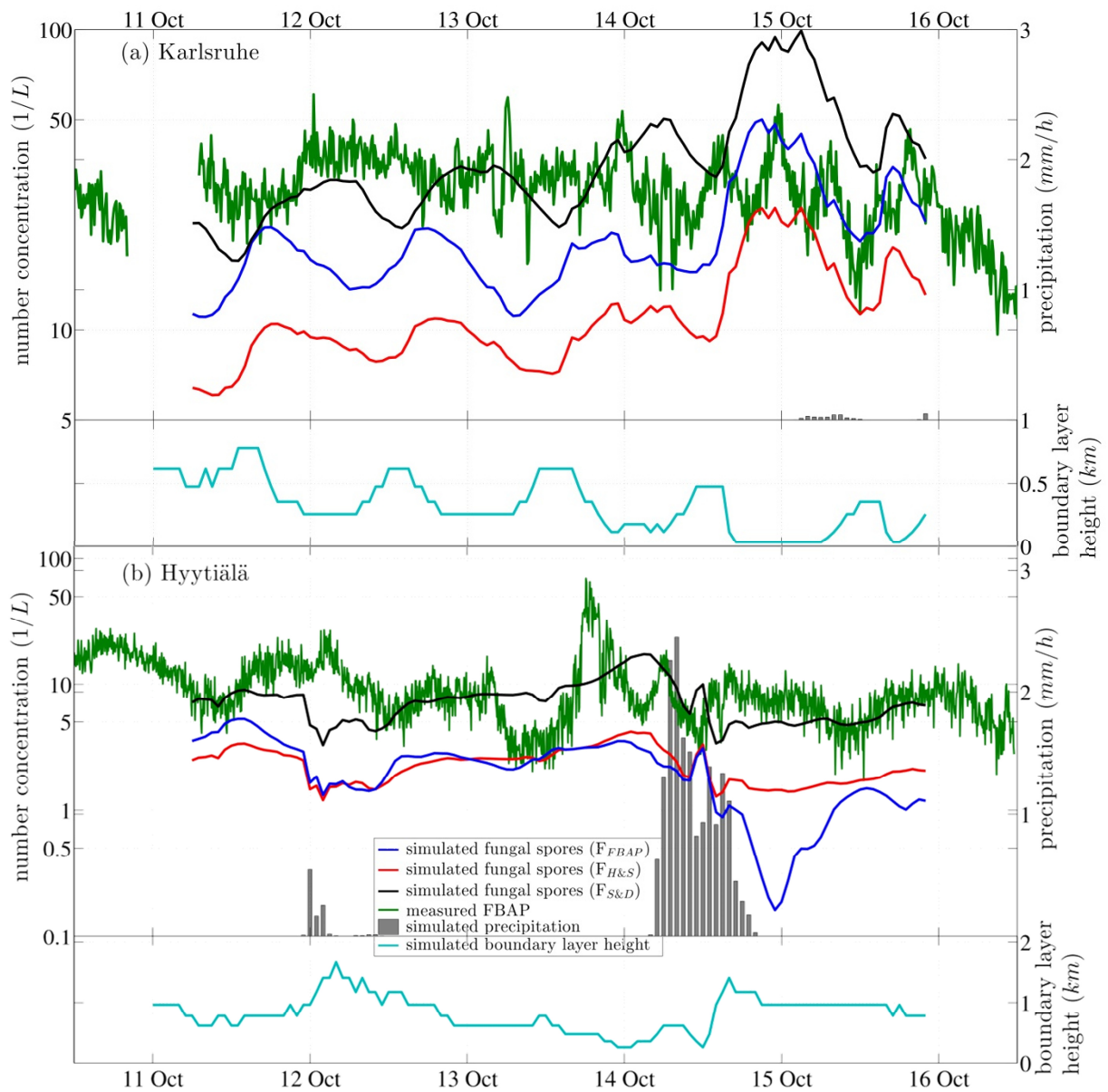
1  
 2 Figure 2. Box-whisker plots of: measured hourly FBAP concentration (open boxes), simulated fungal spore  
 3 concentration emitted by  $F_{H\&S}$  (horizontally hatched boxes),  $F_{FBAP}$  (filled boxes), and  $F_{S\&D}$  (vertically hatched  
 4 boxes) for all case studies. The central mark of each box shows the median, its edges the 25<sup>th</sup> and 75<sup>th</sup>  
 5 percentiles, and whiskers show 5<sup>th</sup> and 95<sup>th</sup> percentiles. Dotes above whisker show outliers (>95<sup>th</sup> percentile).

6



1  
 2 Figure 3. Time series of measured FBAP and simulated fungal spore number concentrations in 1/L together with  
 3 simulated precipitation in mm/h (right axis) and simulated boundary layer height in km (right axis) during the  
 4 case study from 22 July to 28 July 2010 at (a) Karlsruhe, Germany and (b) Hyytiälä, Finland. Simulations were  
 5 performed with three different emission parameterizations:  $F_{H\&S}$  from Heald and Spracklen (2009);  $F_{S\&D}$  from  
 6 Sesartic and Dallafior (2011);  $F_{FBAP}$  from this study.

7

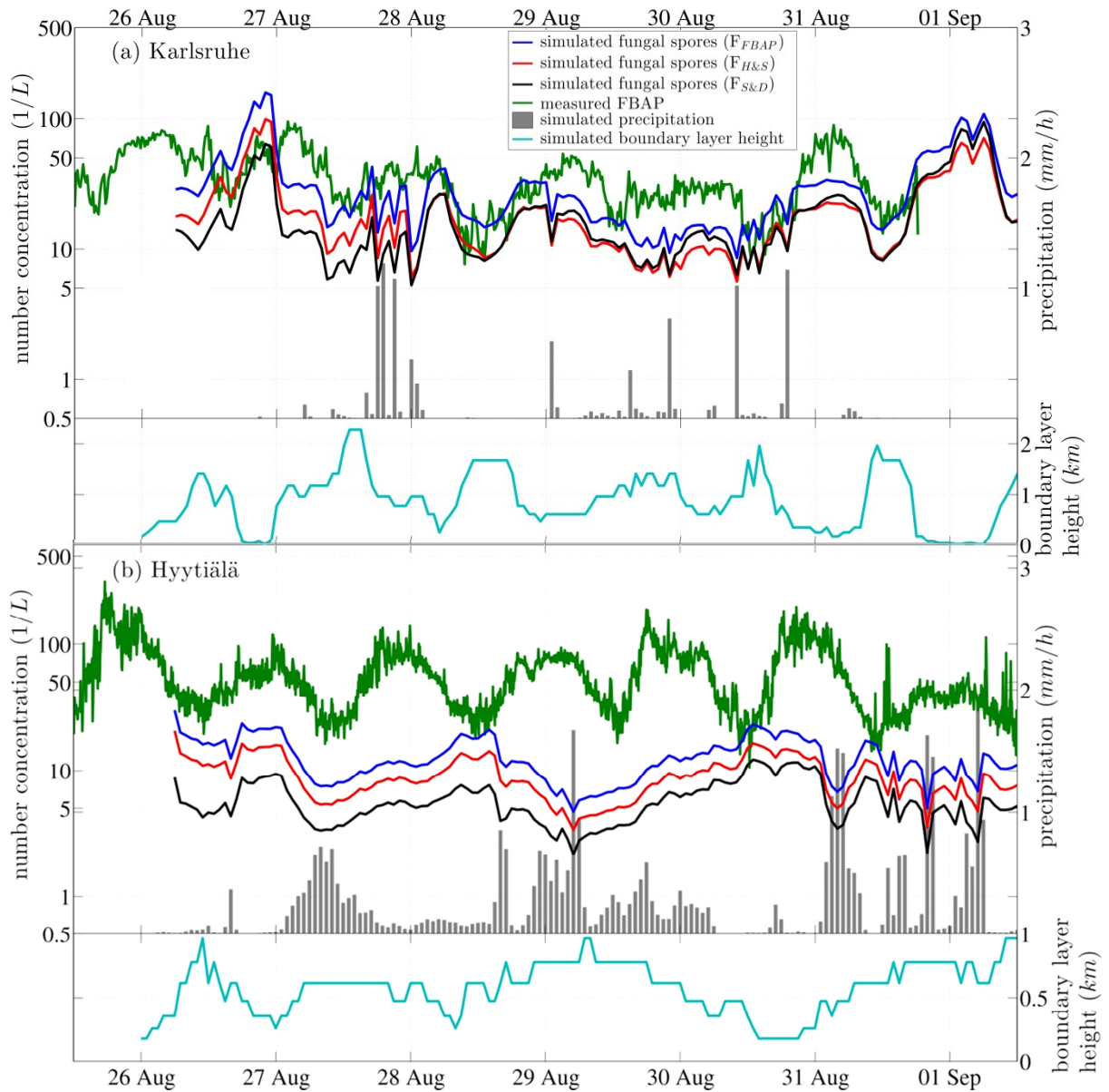


1

2 Figure 4. Time series of measured FBAP and simulated fungal spore number concentrations in 1/L together with  
 3 simulated precipitation in mm/h (right axis) and simulated boundary layer height in km (right axis) during the  
 4 case study from 11 October 2010 to 21 October 2010 at (a) Karlsruhe, Germany and (b) Hyytiälä, Finland.  
 5 Simulations were performed with three different emission parameterizations:  $F_{H\&S}$  from Heald and Spracklen  
 6 (2009);  $F_{S\&D}$  from Sesartic and Dallafior (2011);  $F_{FBAP}$  from this study.

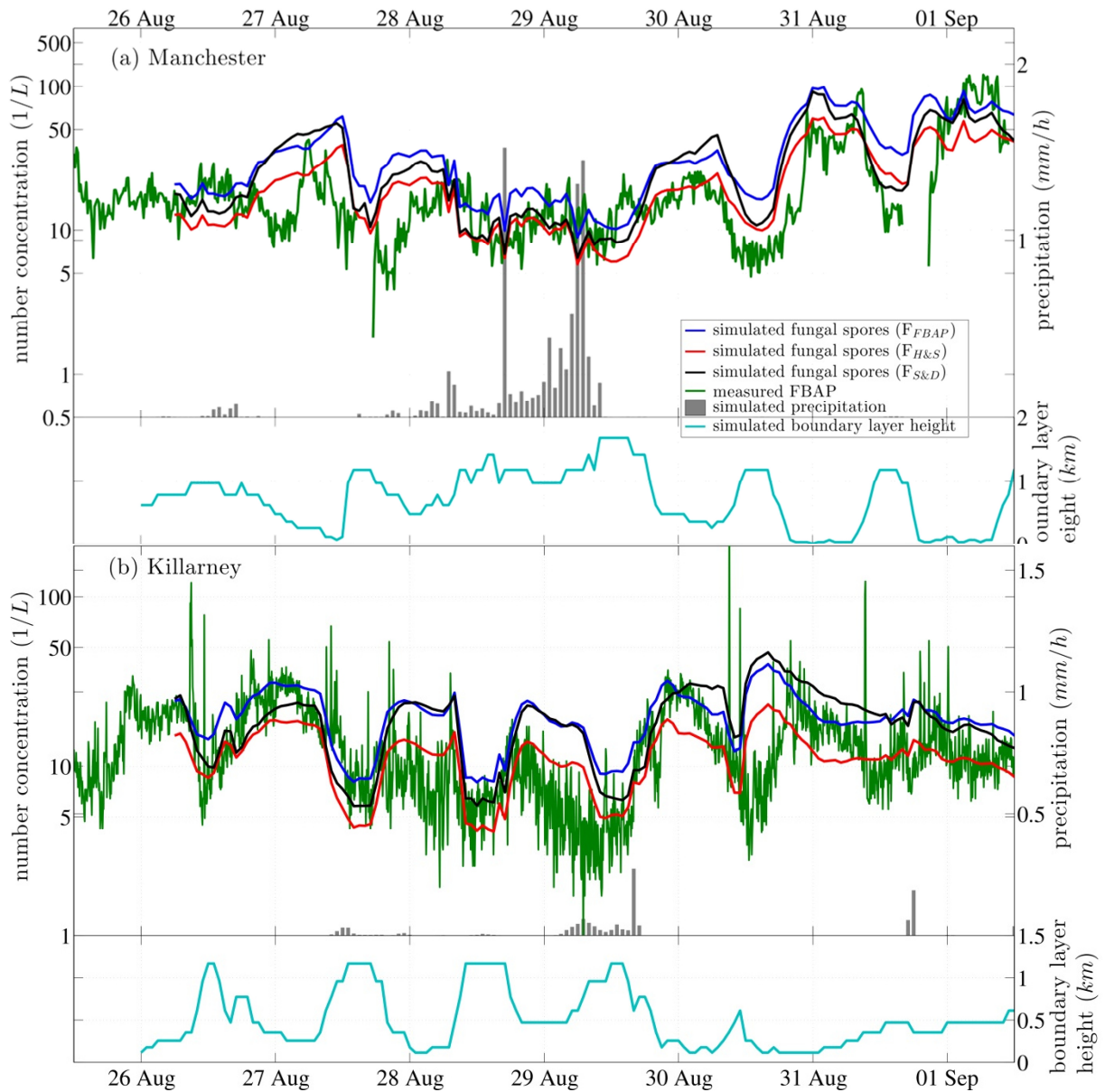
7

8



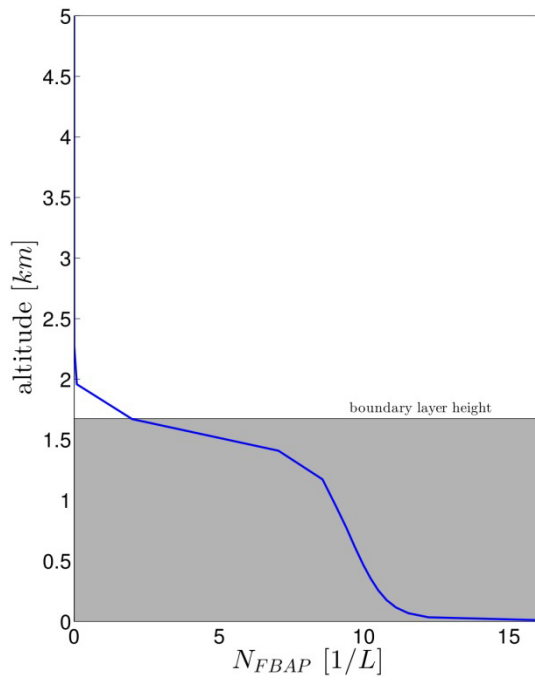
1  
 2 Figure 5. Time series of measured FBAP and simulated fungal spore number concentrations in 1/L together with  
 3 simulated precipitation in mm/h (right axis) and simulated boundary layer height in km (right axis) during the  
 4 case study from 26 August 2010 to 01 September 2010 at (a) Karlsruhe, Germany. (b) Hyytiälä, Finland.  
 5 Simulations were performed with three different emission parameterizations:  $F_{H\&S}$  from Heald and Spracklen  
 6 (2009);  $F_{S\&D}$  from Sesartic and Dallafior (2011);  $F_{FBAP}$  from this study.

7  
 8



1  
 2 Figure 6. Time series of measured FBAP and simulated fungal spore number concentrations in 1/L together with  
 3 simulated precipitation in mm/h (right axis) and simulated boundary layer height in km (right axis) during the  
 4 case study from 26 August 2010 to 01 September 2010 at (a) Manchester, UK and (b) Killarney, Ireland.  
 5 Simulations were performed with three different emission parameterizations:  $F_{H\&S}$  from Heald and Spracklen  
 6 (2009);  $F_{S\&D}$  from Sesartic and Dallafior (2011);  $F_{FBAP}$  from this study.

7

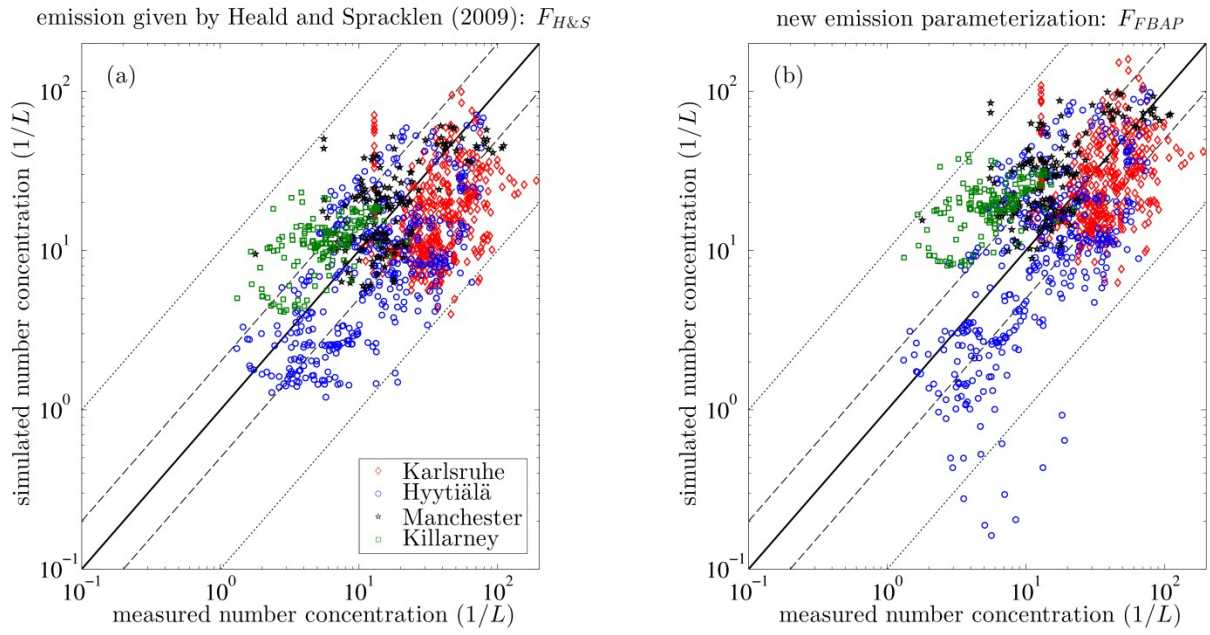


1

2 Figure 7. Exemplary vertical profile of simulated fungal spore concentration within and above the planetary  
3 boundary layer for Karlsruhe at 28 Aug 2010 14 UTC.

4

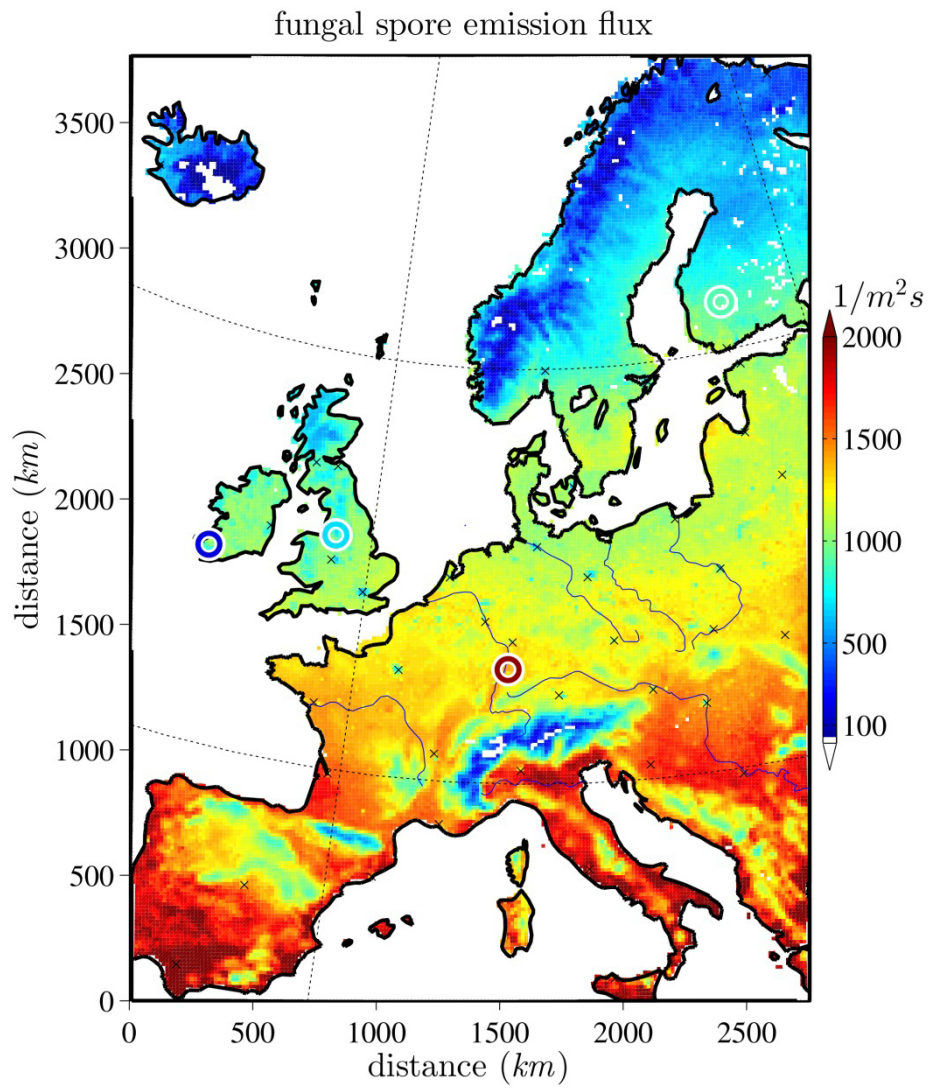
1



2

3 Figure 8. Comparison for all case studies: Measured FBAP number concentrations plotted versus simulated  
4 fungal spore number concentrations (a) based on Heald and Spracklen (2009) emission flux and (b) based on  
5 emission parameterization derived from a multiple linear regression to FBAP concentrations. Solid black lines  
6 represent the 1:1-line, dashed lines the 1:2-line and dotted lines the 1:10-line.

7

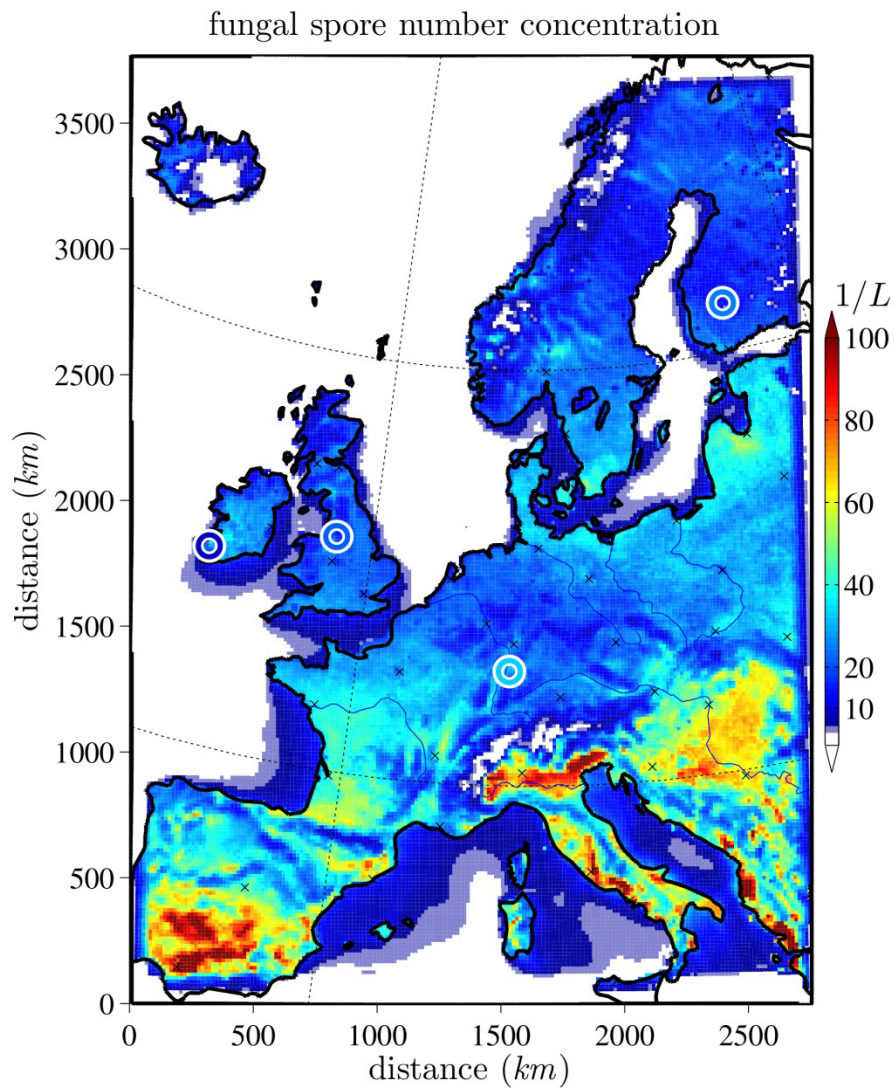


1

2 Figure 9. Average simulated fungal spore emission flux ( $F_{FBAP}$ ) in  $m^{-2}s^{-1}$  from 26 August to 01 September 2010,  
 3 (excluding a spin-up period of 6 hours). White circles indicate the locations of the different FBAP  
 4 measurement time series and the color within the white circles represents the mean emission flux calculated from  
 5 FBAP measurements at each location.

6

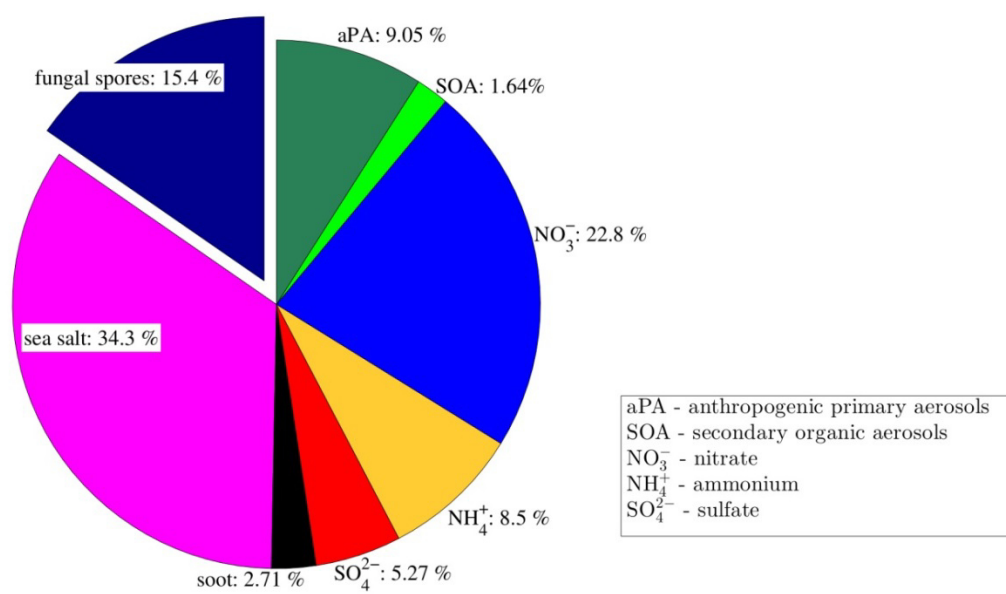
7



1  
2  
3  
4  
5  
6

Figure 10. Horizontally distributed fungal spore concentration in  $1/L$ , emitted by  $F_{FBAP}$ , in the lowest model layer, averaged from 26 August to 01 September 2010 (excluding a spin-up period of 6 hours). White circles indicate the locations of the different FBAP measurement time series and the color within the white circles represents the mean FBAP number concentration measured at each location.

1



2

3 Figure 11. Near-surface chemical aerosol mass composition simulated by COSMO-ART, horizontally averaged  
4 over the land area in the model domain and temporally averaged from 26 August to 01 September 2010  
5 (excluding a spin-up period of 6 hours)

6